Neogene-Quaternary structuring of the Kalaa Khesba Graben, northwestern Tunisia: A push-up inversion structure

Amira Rjiba, Tahar Aifa, Hakim Gabtni, Mohamed Ghanmi, Achref Boulares

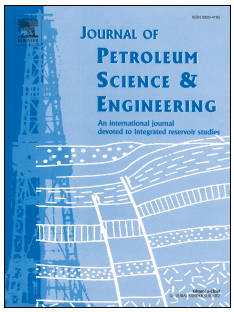

Neogene-Quaternary structuring of the Kalaa Khesba Graben, northwestern Tunisia: A push-up inversion structure

Amira Rjiba, Tahar Aïfa, Hakim Gabtni, Mohamed Ghanmi, Achref Boulares

PII: S0920-4105(19)30853-8

DOI: https://doi.org/10.1016/j.petrol.2019.106432

Reference: PETROL 106432

To appear in: *Journal of Petroleum Science and Engineering*

Received Date: 25 September 2018

Revised Date: 7 August 2019

Accepted Date: 26 August 2019

Please cite this article as: Rjiba, A., Aïfa, T., Gabtni, H., Ghanmi, M., Boulares, A., Neogene-Quaternary structuring of the Kalaa Khesba Graben, northwestern Tunisia: A push-up inversion structure, *Journal of Petroleum Science and Engineering* (2019), doi: https://doi.org/10.1016/j.petrol.2019.106432.

Revised version

Neogene-Quaternary structuring of the Kalaa Khesba Graben, northwestern Tunisia: a push-up inversion structure

Amira Rjiba [1,2,3], Tahar Aïfa [1,*], Hakim Gabtni [3], Mohamed Ghanmi [2], Achref Boulares [4]

[1] Univ Rennes, CNRS, Géosciences Rennes - UMR 6118, Bat. 15, Campus de Beaulieu, F-35000 Rennes, France
[2] Université de Tunis El Manar, Faculté des Sciences de Tunis, UR11ES13 Géomatique Géologie Structurale et Appliquée, 1060 Tunis, Tunisia
[3] Laboratoire de GéoRessources, Centre de Recherches et des Technologies des Eaux (CERTE), Technopôle Borj Cedria, BO 273, 8020 Soliman, Tunisia
[4] Entreprise Tunisienne d'Activités Pétrolières (ETAP), 54, Avenue Mohamed V, 1002 Tunis, Tunisia

[*]Corresponding author: tahar.aifa@univ-rennes1.fr

Abstract

Interpretation of lithostratigraphic, seismic and gravity data from Kalaa Khesba Graben shows (i) lateral and in-depth variation of the lithostratigraphic series, (ii) complex structuring of faulting. Reverse faults affected Paleocene to Quaternary horizons with a duplication of Eocene-Paleocene series occurred at subsurface evidenced within well W6. Isochron, isovelocity and isobath maps, combined with gravity data, show subsurface structures oriented predominantly NW-SE to NS and NE-SW to EW. Faults and horizons on the seismic lines, superimposed to gravity lineaments, reveal negative anomalies occurring at shallow depth. Such features may reflect the existence of low density Neogene-Quaternary series, strike-slips and thrust faults within Kalaa Khesba Graben. Depths deduced from Euler deconvolution solutions vary from 0.5 to 4 km. At subsurface, well log data located in the center of the graben, ensured the presence of Triassic bodies. A model of initiation of Kalaa Khesba Graben through a N160° σ_1 transpression is proposed.

Keywords : strike-slip; pull-apart; lithostratigraphy; seismic reflection; gravity

1. Introduction

Tunisia is located north of the African Continent with a relatively contrasted relief. The geodynamic evolution of this area is controlled by the convergence of Eurasian and African plates. From Late Miocene to Pliocene such convergence produced two orthogonal extensional systems that led to the collapse of the Tell and the Atlas thrust belts in northern Tunisia (Booth Rea et al., 2018). Booth Rea et al. (2018) show that this collapse could be related to the crustal extension in their denudation and its possible relation to deep mantle tectonic mechanisms. Northern Tunisia occupies a transition between both eastern and western Mediterranean basins. Roure et al. (2012) have shown that the mantle lithosphere of the Mediterranean is still locally subducted and recycled in the asthenosphere.

The tectonic history of Tunisia is built as part of the evolution of the Alpine orogeny (Rosenbaum et al., 2002). The complex structures occurring in the Tunisian Atlas are the result of a set of deformations, among which basins that were shaped during its dynamic evolution. Several works (Castany, 1952; Cairo, 1971; Burollet and Rouvier, 1971; Ben Ayed, 1986; Turki et al, 1988; Chihi, 1995) highlight the variety of structures (strike slip, thrust fault, folding, etc.) arranged in the Tunisian Atlas.

Its central part is marked by the presence of several grabens of general orientations NW-SE and WNW-ESE (Burollet, 1991) (Fig. 1a). The Atlassic grabens are associated with strike-slips and evolve more often as pull-apart basins (Chihi, 1995; Bejaoui et al., 2017). Their evolution reinforces the reactivation of the deep NW-SE to EW fault system (Soumaya et al., 2015). The extensional and compressional tectonic phases have affected the northwest of Tunisia since the Mesozoic era (Inoubli et al., 2006). The extension of the Tunisian margin occurred along with the Gibraltar-Messina Transform zone following a NE-SW to EW direction. Large basement-faulting system rejuvenated in dextral, sinistral or normal faults the NW-SE, NE-SW or NS faults, respectively. Southward, the Tunisian Atlas belt is the most important within North Africa. It is attributed to an Eo-Cretaceous structuration. In fact, the Upper Cretaceous-Lower Tertiary extension, followed by the Mio-Plio-Quaternary compression are affected by this Eo-Cretaceous structuration (Martinez et al., 1991). The developed faulting systems play a major role in the migration of saliferous material (Smati, 1983; Perthuisot and Rovier, 1988; Martinez et al., 1991; Chikhaoui, 1998; Chikhaoui et al., 2002; Ghanmi, 2003; Ben Chelbi et al., 2006; Ezzine, 2011). The triggering of the halokinetic movements which occurred during the Upper Cretaceous in various parts of northern Tunisia seems to be due to the major faulting network affecting the Tunisian basement (Perthuisot et al., 1988).

This area is characterized by a series of fault grabens in pull-apart shape located at the eastern end of the Maghreb chains and connected each other by a junction (Chihi, 1995). The geological evolution of this zone is strongly affected by the behavior of the whole North African Alpine (“Maghrebides”) chain and the western Mediterranean. It represents the geodynamic evolution of the Tethys (Bouillin, 1986). Some authors revealed several assumptions on the emplacement chronology of the opening of Kalaa Khesba Graben and the development of its structures. They show that it emplaced prior to the Atlassic folding phase, i.e. during Miocene (Ben Ayed, 1986; Chihi, 1995). The study area shows an alignment of anticline ridges thanks to the reefal or subreefal limestone masses, Albian-Aptian in age (Dj.

Jerissa, Dj. Hmeïma, Dj. Bou El Hanèche, and Dj. Slata) and to broad perched synclines filled by Upper Eocene (Ypresian and Lutetian limestones "Jugurtha Table") to sometimes Oligocene series (Burollet and Rouvier, 1971). One of these fault grabens corresponds with the vast plain of Kalaa Khesba drained by the Oued Serrath and its affluents (Fig. 1b). Kalaa Khesba Graben is limited by both the structures of the Atlassic belt (Tunisian ridge), and the numidian "turbidites", southwards and northwards, respectively. Such numidian "turbidites" widely outcrop in the shape of a thick Oligocene-Lower Miocene clayey sandstone. The interest granted to the geology of this area, started relatively early within the sector of Tadjerouine (Pervinquière, 1903) with a schematic lithostratigraphic cross-section between Koudiat Fretissa and the nummulitic table of Kalaat Senam to evaluate its mining resources (Robaszynski et al., 1998).

Several structures are due to tectonic events that are responsible for the graben opening. The extensional event oriented NE-SW of Kalaa Khesba Graben (Chihi, 1995; Belguith et al., 2011) was initiated during Lower-Middle Miocene. From Late Miocene (Tortonian) to Quaternary the NW-SE transpression was reactivated (Yaich, 1984; Ben Ayed, 1986; Ben Jemiaa, 1986; Delteil et al., 1991; Barrier et al., 1993; Bouaziz et al., 1994, 1998, 2002; Bouaziz, 1995; Chihi, 1995; Zouari, 1995; Dlala, 1996; El Euchi et al., 1998). The present study relates to the emplacement of structures in the faulted graben of Kalaa Khesba and its evolution. In this work, based on data from gravity, 2D seismic and lithostratigraphy within exploration wells W1 to W6, the aim is to:

(i) compute gravity anomaly maps to highlight the depth, orientation of the main faulting system,

(ii) combine seismic and lithostratigraphic data to constrain the infill and evolution of the graben since its emplacement,

(i) use all the available data to identify, characterize the major subsurface structures, including the geometry (edges) of the graben and its tectonic evolution.

2. Lithostratigraphic context

The lithostratigraphic formations of the study area extend, in outcrop, from Triassic to Quaternary. Some formations as the Jurassic series, outcrop only away from this area.

Along the Tunisian Atlas, the Triassic series outcrops in an extrusive context of domes folded into anticlines. Their heart is formed by a gypsum complex, saliferous clays and dolomites, that correspond to the insoluble part of a thick evaporitic formation (Zargouni, 2011). In the study area, dissociated Triassic bodies (Ghanmi et al., 2001) developed in a tectono-sedimentary context in favour of a rifting system. The diapirs are composed of megabreccias of Triassic evaporites deposited in a lagoon environment, hypersaline with fast and rhythmic sedimentation (Lehotsky and Bujnowsky, 1995). Indeed, the Triassic formations could be identified at subsurface in well W6 in the middle of Kalaa Khesba Graben (Fig. 1b).

The Cretaceous series outcrops widely in the area. One finds it present in the form of marls and limestones (Hennebert and Dupuis, 2003). These Cretaceous formations will be described through their various facies: Hameima, Serdj and M'Cherga (Aptian-Albian), Fahdene (Albian-Cenomanian), Bahloul (Cenomanian-Turonian), Aleg (Turonian-Campanian), and Abiod (Campanian-Maastrichtian) Formations.

During the Aptian-Albian stage, the M'Cherga Formation formed by shales, marls, and argillaceous limestones, is presented under three members composed of (i) dark shale alternation with interstratified limestones and sandstones (lower), (ii) shales, marls, and some argillaceous limestones (middle), and (iii) dark schists and marls (upper), respectively. It is represented within well W3 with a thickness of 1170 m.

The Serdj Formation is characterized by massive zoogenous limestones laid out in edges of the fault grabens of Kalaa Khesba and Ouled Bou Ghanem. These limestones also appear at the tops of the diapirs of Dj. Bou El Hanèche, Dj. Jerissa and Dj. Slata (Lehotsky and Bujnowsky, 1995). It is a thick series of bioclastic carbonates which, by places, some reefal constructions occurred. In the SW part of the Tajerouine exploration licence, on well W1, within its border, the Serdj Formation is around 280 m thick (Fig. 2a).

While moving towards well W2 located in the southernmost part of the graben, the Serdj Formation is represented by an approximately 450 m thick pile. The Aptian series is mostly carbonated. In its upper part, there is limestone with some levels of sandstone, clays and levels of crystalline bituminous dolomite rich in stromatolites. The lower part consists of limestone and sandstone alternations.

The Hameima Formation is covered by the basal marl and the schists of the Fahdene Formation containing a Clansayesian fauna (Upper Aptian). The peripheral part of Dj. Jerissa (on the limit of the Tajerouine and Kalaat Senam sheets) is made of alternations of more or less siliceous and dolomitic limestones, marls and brown clays and with hard sandy beds (Burollet, 1956). At the well W3, this formation shows a considerable thickening but one also notes its reduction and complete disappearance on wells W1, W2 and W4, respectively, indicating that the northern zone at the vicinity of well W3 was deeper.

The Fahdene Formation is recognized by limestone-marl series and clays with limestones intercalations. The thickness of the Fahdene member, within well W2, is about 750 m. This formation is also identified within wells W1, W3 and W4, but exists with a very clear thickness reduction which is only of 475 m, 600 m and 280 m, respectively (Fig. 2a). It can also be identified within well W5 (Fig. 2b).

The Bahloul Formation is represented by a double limestone cliff and a primarily Cenomanian marly series. The Aleg Formation is presented in the form of a thick series of gray marls and of shales. Burollet (1956) proposed to delimit an overlying Aleg "sensu stricto" with limestones of Bireno and an Aleg in the broad sense including the base of Annaba and Bireno members. The Aleg terminology is often used to indicate deposits of internal platform type, with formations containing many levels of lumachelle (Falun) formations (Ezzine, 2011). One notes the progressive thickness increase of both members northwards. This thickening is not related to a tectonic phenomenon but rather to a subsidence of the northern part of this area. This subsidence is obviously evidenced by the well log data survey. Thus, one notes within well W1, the lack of both the members. In well W3 (Figs. 2a,b), the Bireno and Annaba members show thicknesses of 135 m and 125 m, respectively. The Abiod Formation is represented by limestones and marls.

The Paleocene-Eocene passage is represented in the study area by three formations:

(i) The El Haria Formation corresponding to gray dark or blackish clays, rich in microfaunas (benthic and planktonic Foraminifera). It is not very resistant to erosion and form the hollow of the valleys or the tender slopes of the reliefs framed by the limestone masses of Abiod and

Metlaoui. The El Haria marls are crowned by the massive flagstone of Metlaoui limestones which forms the Jugurtha Table. One evaluates to 275 m the thickness of the El Haria marls, around the Jugurtha Table (Burollet, 1956). The thickness of this formation decreases southeastwards, probably following erosion within wells W1, W2 and W4 located in the southern part. On the other hand it is present in well W3, where it is represented by clays and a little dolomite on a thickness of 80 m. One also notes the thickening of the El Haria Formation within well W6 (Fig. 2b, Table 1) that can reach nearly 100 m.

(ii) The Chouabine Formation is represented by a succession of marly phosphorites, marls and carbonates alternations.

(iii) The El Gueria Formation is represented by a limestone deposit with benthic microfauna.

The Neogene Formations are characterized by Miocene marls, gypsum and sandstones, by a set of Mio-Pliocene sandstones and of clays and fills the fault grabens of Kalaa Khesba and Ouled Bou Ghanem. The Quaternary Formations are made of rock-falls, very fine and unstratified silts, allowing sometimes some stony intercalations and of alluvia formed by sands, gravels and silts.

3. Description of the exploration wells

The lithostratigraphic data were obtained from the Entreprise Tunisienne d'Activités Pétrolières (ETAP), starting from 6 wells (W1-W6) which were drilled in the study area (Figs. 1-3).

The well W1, established east of the Assilats anticline close to the Algerian border to approximately 45 km NW of Kasserine, presents a lithostratigraphic column, of which the total depth (TD) is of 957 m. This column reaches the Aptian series of Serdj Formation. The five following lithostratigraphic units (from top to bottom) were identified at depths of: (1) 0-140 m: clay with argillaceous marls, argillaceous limestones of Lower Cenomanian age; (2) 140-470 m: clay with marls of Vraconian-Albian age; (3) 470-680 m: marls and argillaceous limestones of Albian age; (4) 680-927 m: clays, limestones and sandstones of Albian-Aptian age; (5) 927-957 m: limestones, dolomites of Aptian age.

The well W2 is located in a sector which presents a lithostratigraphic column of which the final depth reached is of 2298.5 m. The five following lithostratigraphic units (from top to bottom) were identified at depths of: (1) 0-60 m: Turonian marls; (2) 60-800 m: Cenomanian dark marls and limestone levels; (3) 800-1350 m: Lower to Middle Albian marly clays; (4) 1350-1960 m: Aptian clays with intercalation of limestones; (5) 1960-2000 m: Barremian marly clays; (6) 2000-2298 m: Hauterivian calcareous sandstones.

The well W3, located in the area of Tajerouine (Fig. 2b), presents a lithostratigraphic column reaching the Aptian series of Serdj Formation, with a final depth of 3700 m. The nine following lithostratigraphic units (from top to bottom) were identified at depths of: (1) 0-100 m: Ypresian marls; (2) 100-600 m: Turonian-Santonian marls and limestones; (3) 600-870 m: Turonian marls, clays and limestones; (4) 870-920 m: Cenomanian-Turonian limestones; (5) 920-1600 m: Albian-Cenomanian limestones and marls; (6) 1600-2100 m: Albian limestones and marls; (7) 2100-2460 m: Aptian limestones and clays; (8) 2460-2500 m: Gargasian limestones; (9) 2500-3700 m: limestones, marls and clays of unspecified Gargasian-Cretaceous age.

The well W4, drilled to evaluate the hydrocarbon potential of the northern zone of Thala, presents a lithostratigraphic column of 2011 m. The five following lithostratigraphic units (from top to bottom) were identified at depth: (1) 0-250 m: Campanian-Maastrichtian limestones, marls and argillaceous limestones; (2) 250-1200 m: Turonian limestones; (3) 1200-1320 m: Cenomanian-Turonian argillaceous limestones; (4) 1320-1600 m: Cenomanian limestones; (5) 1600-2011 m: Triassic dolomites.

The well W5, located on the northern edge of the Rouhia Graben, presents a lithostratigraphic column of 1119.6 m and thus stops in the Aptian series of Serdj Formation. The three following lithostratigraphic units (from top to bottom) were identified for depths at: (1) 0-600 m: alternation of the marls and limestones Albian in age; (2) 600-1040 m: Albian-Aptian massive limestones and limestones and marls alternations; (3) 1040-1119.6 m: gray to beige dolomites with inserted dark to black clays Aptian in age.

The well W6, located at 10 km SE of Tajerouine is drilled in the eastern part of the graben. It reaches a 2064 m depth (Table 1) to stop on top of the Triassic saliferous series. The seventeen following lithostratigraphic units (from top to bottom) were identified at depths of: (1) 10-307 m: Pliocene sands, clays and conglomerates; (2) 307-390 m: Tortonian-Messinian clays and sands; (3) 390-1000 m: Langhian-Serravallian gypsum and sandy clays; (4) 1000-1200 m: alternation of dolomites, marls and of clays, Lutetian in age; (5) 1200-1240 m: Tortonian-Messinian sandy clays; (6) 1240-1350 m: Lutetian limestones; (7) 1350-1390 m: alternation of Ypresian dolomites and marls; (8) 1390-1420 m: Danian marls; (9) 1420-1510 m: alternation of Ypresian dolomites and marls; (10) 1510-1570 m: Lutetian marls; (11) 1570-1580 m: alternation dolomites and marls, Ypresian in age; (12) 1580-1650 m: Lutetian limestones; (13) 1650-1700 m: alternation dolomites and marls, Ypresian in age; (14) 1700-1800 m: Thanetian marls; (15) 1800-1900 m: Campanian-Maastrichtian limestones; (16) 1900-2000 m: Santonian-Campanian marls with levels of limestones; (17) 2000-2064 m: Turonian-Santonian gypsum.

4. Structural context

The structuring of the Atlassic foreland seems to be relatively simple. It is characterized by folds and faults of varied nature and distribution (Ben Ayed, 1986). The Atlassic grabens form a significant structural entity in front of the North African Alpine chain. Their evolution is related to that of the central Mediterranean (Chihi, 1995). According to Castany (1952) and Richert (1971), these normal fault bounded grabens are differentiated during the compressive phase and would be posterior to major folding. For Caire (1977), the result of the opening of these grabens is due to the distensive faulting system within the sedimentary cover during deep shearing at the basement. The grabens oriented NW-SE are distributed within a pull-apart collapse system along with an EW dextral shear (Chihi, 1995). Their evolution reinforces the reactivation of the deep NW-SE to EW fault system (Soumaya et al., 2015). The opening of these grabens due to the extensional faulting system of the sedimentary cover (Caire, 1971) is post-folding (Castany, 1952; Richert, 1971; Ben Ayed, 1975; Chihi, 1995; Ben Romdhane et al., 2006; Belguith et al., 2011).

The study area extends northwestwards and includes NE-SW oriented folds resulting from the Aurès (Castany, 1952). It is marked by a hydrographic network of Oued Serrath in Kalaa Khesba Graben which is a good indicator to determine the lineament directions of the main

tectonic faults (Fig. 1b). It presents a suite of “en echelon” anticlines and synclines oriented NE-SW (Ben Ayed, 1986), with brittle faults and saliferous material. The diapiric structures are often located on the edges of the grabens faults. The injection of the Triassic evaporites extends to several kilometers, forming hence shallow anticlines (Dj. Jerissa, Bou El Hanèche). The propagation of this kind of folding is ensured by the “decollement” of these Triassic series (Ezzine et al., 2008). It is mainly the case of Kef El Jegaga - Dj. Slata Diapir which is an anticlinal structure of Atlassic direction (NE-SW) corresponding to one of the Triassic body structures (Smati, 1986 ; Perthuisot and Rovier, 1988 ; Chikhaoui, 1998 ; Ghanmi, 2003). Such Triassic extrusions are aligned into bands of NE-SW direction (Ben Chelbi et al., 2006). In the upper part of Kalaa Khesba graben within Dj. Slata one may observe a centrifugal inversion of the host series during the emplacement of the Triassic material (Perthuisot et al., 1998). The Triassic outcrops of the diapirs zones show a certain complexity in the relationships between saliferous material and its host rock (Chikhaoui et al., 2002). The study area is characterized by major NW-SE and NE-SW faults. Both grabens of Kalaa Khesba and Kalaat Senam are delimited by N140°-160° conjugate faults combined with the N80° shear (Ben Ayed, 1986). The main faults are oriented WNW-ESE (Lehotsky and Bujnowsky, 1995). Kalaa Khesba Graben is represented by two branches, a NW-SE limited by “en echelon” faults of N140°-170° direction and an EW corresponding to Ain El Kseiba Depression located at the south of Bou El Hanèche (Chihi, 1995). According to reverse and strike-slip faults, the tectonic analysis shows a main NW-SE compression to the Atlassic folding phase (Ben Ayed, 1986).

5. Geophysical data

5a. Seismic data

The seismic reflection data were obtained thanks to the contribution of ETAP. The profiles of the seismic surveys were carried out by ETAP: EK1 in 1945, OR1 in 1967, OSR in 1969, ASS1 in 1970, TH1 in 1981, and Semda in 2011 in the Kalaat Senam Graben faulting. Six exploration well surveys were taken into account in this study : W1 (Aquitaine Tunisia), W2 (Tunisia Exploration), W3 (Compagnie Générale de Géophysique), W4 (North-African Petroleum Company), W5 (Hydraulic Equipment), and W6 (Mosbacher Tunisia LLC) (Table 2). These seismic lines were established following several seismic missions with acquisition parameters and varied treatment stages. Among these lines is the line L1 that is perpendicular to the graben. It was carried out by Mosbacher Tunisia LLC in May 1995. Its calibration was carried out using the studied well W6 (Table 2) which cross-cuts it and while based itself on a time-depth curve. The processing sequence on the data profile is ensured using a replacement speed of 2000 m/s and a refraction speed of 2534 m/s (overburden velocity of 1 km/s). The second line L2 is parallel to Kalaa Khesba Graben, with the same velocities as for line L1. Coordinates limits of both sections L1 and L2 are (456712/3953934) to (467072/3948992) and (465388/3954415) to (470507/3947307) in UTM WGS84, respectively. The line L3 is a composite line of L1 and L2.

5b. Gravity data

High-resolution gravity data in the northern Tunisian Atlas were collected by the Office National des Mines (ONM, 1997) with an average spacing of 1 km. The gravity data cover the

Kalaat Senam - Kalaa Khesba map at the scale of 1/50,000. The data acquisition was carried out through gravity survey within the framework of the establishment of the gravity Atlas of Tunisia. A general sight of gravity in the study area of Kalaat Senam - Kalaa Khesba was conducted using a Worden type gravitymeter. It is composed of 63232 gridded points. The gravity anomaly maps were calculated according to WGS84 UTM Z32 N system. The adopted projection is Lambert North using the ellipsoid of Clark 1880 and the Carthage datum. The gravitymeter used for the survey is a Scintrex CG5 type. An adopted correction utilizes the theoretical gravity obtained starting from the equation defined by the International Association of Geodesy (1971) with zero sea level as a reference. The maps at the scale of 1/50,000 provided by the Office of Topography and Cartography of Tunisia were used, after digitalization, in the computing process of the topographic corrections. For the whole of the corrections carried out, the selected compensation density is 2.4 g/cm^3.

The choice of this value results from the comparison of the results of several methods. The good correlation between the density of Nettleton and the densities measured made it possible to choose a regional density of 2.4 g/cm^3.

6. Geophysical data processing

Processing of the seismic data was realized at ETAP using the “SMT” software (Kingdom software, 2015). The details of the seismic data processing is here out of the aim of the subject, so will not be developed. One starts with the identification of the horizons through the seismic calibration, and one refers to the seismic coring of the well compared to the data of vertical seismic profile (VSP). This pointing of the horizons was established while following a seismic horizon laterally, along a seismic profile and at the same time one traces the faults according to their geological significances. After the identification of these horizons on all the seismic lines, one recorded and marked the time values on the various shot points of the seismic position. The isochronous curves thereafter were drawn. One passes, thereafter, with the correlation of the faults in order to obtain an isochron map expressed in Two Way Time (TWT, s). The production of an isovelocity map consists in calculating the mean velocities within wells for each roof of the formation to interpret. The seismic data processing made it possible to improve the recordings for their interpretation. The transformation of the seismic answers at the profiles interpretation level made it possible to give a representation of the subsurface, from where a relationship can be established between the geometry of the major geological structures deduced from the seismic answers and the regional geology.

Processing of the gravity data was realized using Geosoft software (Geoscoft Inc., 2013). It is a question of carrying out the application of operators to extract information on the subsurface structures. The separation of regional and residual anomalies were made using several methods from where the choice of regional anomaly which will fix the nature and the profile of the residual anomaly. Such methods are based on graphic smoothing on the contours, calculation of the regional anomaly analytically or by application of a filter, and calculation of the effect of the source to eliminate, i.e. if its geometry and its density are known in order to withdraw it from the Bouguer anomaly (modeling). We used filters such as polynomial regression, spectral analysis and upward continuation to determine the regional anomaly (see e.g. Gabtni and Jallouli, 2017).

The upward continuation allowed to filter the short wavelengths. It produces a regional anomaly that is subtracted to Bouguer anomaly to obtain the residual anomaly. The expression of the regional anomaly is (Jacobsen, 1987): $h_{reg}(k) = (1 + \frac{S_{res}}{S_{reg}})e^{[2k(z_{reg} - z_{res})]^{-1}}$

where k : norm of the wave vector; $S_{res,}\, S_{reg}$: intensity of the source (residual and regional, respectively); $z_{reg} > z_{res}$, z : depth.

The horizontal gradient allows to have narrower transformed anomalies, by amplifying the high frequency signal corresponding to less extended and surface sources. The Euler deconvolution is a method which authorizes the horizontal localization as well as the estimate depth of the geological objects. Indeed, it depends primarily on the spacing grid between profiles, the size of deconvolution windows, and the structural index (Reid et al., 1990).

7. Results

7a. Seismic interpretation

The interpretation of the seismic profiles L1, L2 and L3 allows to follow the lateral (side) and vertical evolution of the sedimentary sequences and to detect the role of tectonics in the basin evolution. Profile L1, oriented SW-NE revealed a synclinal form limited by a bordering fault to the west (Fig. 4). The ages of the geological formations extend from Triassic to Quaternary, but with a lack of the Jurassic formation, and a lateral variation of the facies and the thicknesses. The main reflectors extracted from the seismic section L1 (Fig. 4b-c) are at: (i) the SW, roofs of Bireno (Turonian), Serdj (Aptian), and evaporitic (Upper Triassic) Formations, (ii) the NE, roofs of Segui (Pliocene), Oum Dhouil (Miocene), Chouabine and El Gueria (Eocene), El Haria (Paleocene), Bireno (Turonian), Serdj (Aptian), and evaporitic (Upper Triassic) Formations.

In this seismic section one can observe (Fig. 4b,c): (i) a change in the reflector shape of the sedimentary layers which indicates that horizons of the Segui, Oum Dhouil, El Gueria, Chouabine, and El Haria Formations stop onto fault F1 (Mahjouba Fault) and do not continue southwestwards. On the other hand, the Cretaceous series (Bireno and Serdj) and those of the Triassic end with a clear thickness variation (Fig. 4b). (ii) a duplication of the El Gueria, Chouabine and El Haria horizons which are affected by F2, F4 normal and F5, F6, F7 reverse faults, respectively. The existence of an overlapping is thus evidenced within the center of Kalaa Khesba Graben.

In the interpreted seismic section (Fig. 4c), several faults were presented from F1 to F9. The F2-F9 faults exhibit a positive flower structure characteristic of strike-slips. They occupy the graben depocenter. The rooting of this flower structure deepens and reveals indices of reverse faulting system.

The seismic profile L2 oriented NW-SE, passes parallel to Kalaa Khesba Graben. The ages of the geological formations extend from Triassic to Quaternary, also showing a lateral variation of the facies and thicknesses. The principal reflectors on the seismic section L2 oriented NW-SE (Fig. 5b) are: the Segui (Pliocene), Oum Dhouil (Miocene), Chouabine and El Gueria (Eocene), El Haria (Paleocene), Bireno (Turonian), Serdj (Aptian), and evaporites (Upper Triassic) Formations.

This seismic section (Fig. 5b,c) shows: (i) an erosional truncation, (ii) a continuity of the horizons on all the profile with a clear variation thickness towards the SE, (iii) the same duplication of the El Gueria, Chouabine and El Haria horizons as for section L1.

The seismic profile L3 is a composite line of L1 and L2 (Fig. 6). It presents the various faults and interpreted well in both lines. It shows on the well W6, with a good precision, the Neogene-Quaternary overlapping indicated by the set of reverse faults as well as a large syn-graben faulted fold. The structural evolution of the grabens as well as the major faults can be better illustrated using maps of the various horizons. In our study area, one followed the roof evolution of the Aptian Serdj Formation: From the isochron map (Fig. 7), in the center one distinguishes a deepening of the graben which translates an overall dip from west to east. The isocontours vary between 0.413 s and 2.080 s in two way time (TWT). This map reflects a clear and well individualized morphology. It makes it possible to distinguish three high structures: Semda (isocontours from 1. 4 s to 1.6 s TWT), Thala and Mahjouba (isocontours from 1.10 s to 1.3 s TWT), as of the major zones (graben) whose isochrons vary from 1.6 s to 1.9 s TWT. The in-depth conversion of the isochron maps to the roof of Serdj Formation and the isovelocity (Fig. 8) and isobath (Fig. 9) maps were also carried out. The isobath map shows curves whose values vary from 727 m to 3441 m (Fig. 9). It allows to identify the same faults network NW-SE to NS, NE-SW to EW oriented and especially the same prospects (Semda, Thala and Mahjouba) in which the isocurves vary from 2815 m to 1457 m. This map shows a thorough part on the Kalaa Khesba Graben of which the depths vary from 2710 m to 3441 m with prevalence of faults oriented NW-SE, NE-SW and EW.

7b. Gravity interpretation

The gravity method enables us to determine density anomalies and interpret the subsurface structures. The computed Bouguer anomaly map is presented by values varying from -42.762 mGal to -20.029 mGal (Fig. 10). The map thus established shows the positive Bouguer anomalies with values going from -27.342 mGal to -20.029 mGal superimposed on maximum amplitudes such as for example in Dj. Jerissa and Dj. Bou Afna. Negative anomalies are represented by the weakest anomaly, the values are about -42.762 mGal to -32.157 mGal. These anomalies are lengthened according to a NNW-SSE direction in agreement with the extension of Kalaa Khesba Basin. The regional anomaly is subtracted to Bouguer anomaly to obtain the residual anomaly. The regional map was obtained with a polynomial of order 3. It presents values varying from -43.051 mGal to -22.528 mGal (Fig. 11). The residual map of order 3 (Fig. 12) has been selected because it reflects the expression of the surface sources characterized by short and medium wavelengths. It represents mainly the variations of density including thickness and density variations of the sedimentary rocks. On this map, a negative residual gravity anomaly is distinguished, whose maximum amplitude is ranging between -15.674 and 5.714 mGal (Fig. 12). One also notes (i) a migration of the localized positive zone in the western side border of Kalaa Khesba Graben, which is a NS strong amplitude anomaly centered on Dj. Bou Afna. (ii) a lengthening of the negative anomaly according to a NNW-SSE direction, parallel to Kalaa Khesba Basin, corresponding to Quaternary alluvia.

To estimate the sources depths, a power spectrum was computed (Spector and Grant, 1970). From Bouguer anomaly map data, the average depth for each slope was analyzed by least squares (Gabtni and Jallouli, 2017). If the unit of frequency is in cycles/km, the average depth

of each source z related to each segment is: $z = -\frac{4\pi}{s}$, where s is the slope of the straight line obtained by least squares.

In its low frequency part (lower than 2.5 cycles/km), the power spectrum shows three strongly marked slopes due to the major deep sources (Fig. 13). The main sources have their average depths at $z_1 = 3.2$ km, $z_2 = 1.65$ km and $z_3 = 0.8$ km.

The horizontal gradient expresses the rate of lateral variation of the gravity field (Blakely and Simpson, 1986). The Horizontal gravity gradient (HGG) map (Fig. 14) delimits the vertical and lateral sources locations to distinguish the various directions of structures and faults at subsurface (Gabtni and Gouasmia, 2013). In our study three families of faulting directions, NW-SE, NNW-SSE to NS and NE-SW to EW appear, where the NW-SE and EW directions prevail. The bordering faults of Kalaa Khesba Graben, as well as the layouts of alignments of faults networks whose anomalies vary between 0.00021 mGal/m and 0.00418 mGal/m have a NW-SE direction, with prevalence towards the NS. On the Kalaat Senam syncline, NE-SW and EW alignments occur.

The technique of Euler Deconvolution solutions was also used to estimate the depths of the sources (Reid et al., 1990). The expression of the Euler equation is given by Thompson (1982):

$$(x - x_0)\frac{\partial \Delta T}{\partial x} + (y - y_0)\frac{\partial \Delta T}{\partial y} - z_0\frac{\partial \Delta T}{\partial z} = -N\Delta T(x, y)$$

with x_0, y_0, z_0 : local coordinates, ΔT : Intensity of the magnetic field, N: structural index.

By using this technique, one may identify the Euler solutions of the various underlying structures within the sedimentary basin (Fig. 15).

These solutions were calculated starting from the following Euler parameters: Structural index: SI=0, Dimension of the window: W = 10, Tolerance: Z = 15%.

The Euler Deconvolution map is helpful to determine the depth of various geological bodies. The rooting of the sources deduced by the Euler Deconvolution are at depths estimated between 0.5 and 4 km. They would correspond to the existence of faults oriented NW-SE to NS and NE-SW to EW.

8. Discussion

Assumptions on the chronology of the tectonic events during the emplacement and the evolution of the grabens within the central Atlas of Tunisia were proposed (Ben Ayed, 1986 ; Chihi, 1995 ; Dlala, 2001). Some of the authors tried to explain the structure of the grabens edges (Caire 1971 ; Burollet et Rouvier, 1971 ; Ben Ayed, 1986 ; Chihi, 1995 ; Gabtni et al., 2016). The northern part of central Tunisia is occupied by several grabens oriented NW-SE and WNW-ESE (Burollet, 1991). The main deformation phase, corresponding to the Alpine compression, related to the Africa-Eurasia convergence, is Serravalian in age and oriented N160°. It is followed by the Messinian rifting phase which induced the NW-SE opening of grabens in our study area, summarized by Bouaziz et al. (2002).

The first tectonic events observed are Triassic in age and correspond to the NS compressional event related to the opening phase having involved an instability of the sedimentary basement. They induced subsident zones (Ezzine, 2011). From Lower Cretaceous to Campanian-Maastrichtian a distensive to transtensive deformation is recorded (Dlala, 2001). The first

compressive pulsations occurred only during the Upper Cretaceous, i.e. at the Maastrichtian (Ezzine, 2011). But from late Cretaceous to Miocene developed distensive structures accompanied by "decollement" and blocks tilting. During the Paleocene-Eocene a major compressional phase, N160° oriented, inducing folds and fractures, occurred (Zargouni, 1984). The presence of an unconformity within the Lutetian sediments suggests an erosional truncation of Bartonian to Burdigalian sedimentary deposits. In fact, such an unconformity corresponding to the marine Langhian-Serravalian transgression was recognized in well W6 (Martinez and Truille, 1987; Belghithi et al., 2016) (Table 1, Fig. 16). The major Atlassic phase, Upper Miocene (Tortonian) in age, is the major compressive tectonic event inducing strike-slips and overlaps. During Miocene, the Tunisian grabens would then be the first evidences within the Alpine foreland of the overlaps jam (Ben Ayed, 1986). Whereas during Upper Pliocene transtensive tectonics was set up (Ben Ayed, 1986). While during Quaternary compressive cycle N160° to NS oriented with reactivation of the preexistent structures acts on the Atlassic direction folds (NE-SW). The extensional and halokinetic movements recorded may explain the evolution of the grabens. From stress field inversion of 123 focal mechanisms coming from different sources of Tunisia, Soumaya et al. (2015) found a first-order stress field oriented horizontally N150°. Such stress field is compatible with a transpressional regime in the Atlassic foreland, reactivating hence the NW-SE fault system (Chihi, 1995). Kalaa Khesba L1 cross-section shows (i) an injection of evaporites along the F1 fault which limits this graben westwards thus (ii) a Miocene in age reactivation of the preexistent Mesozoic extensional faulting system occurred, as indicated also by Belguith et al. (2011). It suggests that the deformation leading to the rifts observed is of regional scale dated at Late Miocene to Quaternary. Although, the Quaternary formations seem to post-date the rift system. (iii) Ezzine (2012) identified four angular unconformities as well as duplication of El Gueria, Chouabine and El Haria series associated with the formation of duplexes allow to draw nested structures. The interpreted seismic profiles (Figs. 4-6) show the Paleocene-Eocene age series (El Haria, Chouabine and El Gueria Formations) recognized within W6 well log (Table 1) and confirm such a duplication (Fig. 16).

The normal fault F1, separates the Mesozoic and Tertiary-Quaternary formations (density contrast of 0.35 g/cm^3), west- and east-wards, respectively. Gabtni et al. (2016) used gravity and seismic modeling to show that it dips 45° to the east. In addition, the NW-SE grabens exhibit at their SE boarders major EW dextral strike-slips (Chihi, 1995), associated to "en echelon" folds and megastructures (Chihi et al., 1992). As a consequence, anticlinal structures oriented NE-SW were moved southeastwards and southwards (Gastany, 1952). In addition, the interpretation of the present gravity, seismic and lithostratigraphic data indicate that

(i) the EW dextral shear is at the origin of Kalaa Khesba Graben structuration,

(ii) this shear results from reverse and normal faults during the regional extensional phase which is the resultant of a transtension having controlled the syn-graben tectonics,

(iii) the activation of the faults passing by the well W6 seems to have had a major impact on the graben structure.

According to well data (Figs. 2) the structuration of Kalaa Khesba Graben can be constrained as follows: (i) the Miocene Oum Dhouil Formation unconformably lays on the Eocene Cherahil Formation, suggesting a strong erosion which would have removed the Oligocene Formations (Table 1). (ii) the Aptian Serdj Formation, with carbonated predominance, and the

Hameima Formation show a considerable thickening, in particular within wells W1-W3 (Fig. 2a). However, a complete disappearance of the Hameima Formation is noticed within well W4. It is deduced that the northern zone, in the vicinity of well W3, was deeper and was not emerged for the period of sedimentation of Serdj Formation. (iii) the Aleg Formation, composed of two members (Annaba and Bireno), consists of a continuous thickening northwards. This thicknening is not due to a tectonic phenomenon only but to a subsidence of the northern part of the study area. This subsidence is evidenced by well log surveys data (wells W2-W4) (Fig. 2a). (iv) the layers of the Paleocene El Haria Formation are missing in some wells probably following erosion, noted in wells W3 and W6 (Fig. 2b). All the Jurassic layers are also missing. The composite seismic section L3 (Fig. 6) cross-cutting Kalaa Khesba Graben according to SW-NE and NW-SE directions and calibrated by well W6 offers invaluable information at the time of the deformation. It shows a duplication of the Paleocene-Eocene series with the existence of a possible positive flower structure. An overlapping related to the EW strike-skip, located within the Neogene-Quaternary Formations passing by well W6, occurred (Fig. 6). The analysis of the computed isochron, isovelocity and isobath maps as well as the gravity data shows a predominance of major faults according to directions NW-SE, NNW-SSE to NS and NE-SW to EW. They are exhibited on the HGG map of Kalaa Khesba and Kalaat Senam (Fig. 14) indicating clearly the main bordering faults with their dips. They are probably related to EW “en echelon” dextral faulting system, i.e. related to a simple pull-apart system.

According to Euler Deconvolution map, the depths values of these faults vary from 0.5 km to 4 km (Fig. 15). This is in agreement with the depths deduced from the power spectrum (Fig. 13), the isobath map (Fig. 9), and the vicinity or within well W6 (Fig. 16). The whole of these results, based on gravity and seismic data, lead to a possible geological interpretation of the area through a simple 3D model (Fig. 17). It shows that the NW-SE compressive Miocene phase inducing strike-slips triggering this pull-apart basin and its further development (Fig. 17a). It seems to be responsible for blocks tilting and occurrence of anticlinal and synclinal structures affected by numerous normal, reverse or strike-slip faults. This faulting system, particularly within the anticline beneath well W6 (Fig. 16), reactived and affected the prevailing structures. It could be considered as a thrust-faulted fold or shear fault-related fold (Fig. 17). The extension of ENE-WSW direction guided the formation of structures into grabens, half-grabens and vast synclines. These grabens evolved through a series of compressional and extensional periods according to a pull-apart system. The seismic data show the existence of Triassic bodies raised at subsurface, by density contrast, owing to faults and fractures. Consequently, the halokinetic movements seem to be at the origin of the evaporitic flows as well as of the active faults.

In a paper regarding push-up structures, Pace and Calamita (2014) have demonstrated that the geometry of such structures is related to transpressional reactivation of pre-existing normal faults. The grabens of the Tunisian Atlas, which are classified as pull-apart basins, deep enough for the maturation of the organic matter, represent an objective of hydrocarbons exploration. Indeed, Kalaa Khesba quickly developed through a fast subsidence accommodated by such faulting system. The large accumulation of sediments, in particular the main Serdj Formation which is potentially a favorable reservoir to the structural and stratigraphic traps, as mentioned in the isobath map (Fig. 9).

9. Conclusion

Tectonics undergone by Tunisia is mainly represented by Atlassic folding of Alpine type and stable platforms (Burollet et Rouvier, 1971). This study allowed to delimit the Kalaa Khesba Graben which shows differences in thickness and geometry of the sediments. These differences are the consequences of the major compressive phase which is at the origin of the activation and/or reactivation of the faults.

The whole of the gravity and seismic studies available on the northwestern Tunisian provided accurate information on (i) the succession of the horizons within the grabens, (ii) the main faults directions having contributed to its current configuration. They thus allowed to contribute to the structuring of this zone marked by fault grabens. It is now possible to define the tectonic and sedimentary evolution of the area. During Mesozoic and Cenozoic eras, pull-apart basins opened (Fig. 1b). This period is also highlighted by tectonic events which gave varied structural units, e.g. saliferous structures, brittle faults in major accidents and box folds. The evaluation of the geological and subsurface (gravity and seismic reflection) data can lead to the five following conclusions: (i) the activation of the bordering grabens faults; (ii) the F1 fault which borders the graben westwards, considered as a major fault, is used as supports with branches of faults leading to a positive flower structure, characteristic of a strike-slip; (iii) Kalaa Khesba graben is characterized by a negative anomaly with very low depth translating the presence of a series of low density. The orientation of these anomalies helps to identify the major structural directions of the area. (iv) both sides of the graben are oriented roughly NW-SE. Compared to Bouguer anomaly map (Fig. 10), the 3rd order residual anomaly map (Fig. 12) shows more details related to pull-apart basins. (v) the opening of Kalaa Khesba Graben occurred through an NE-SW extensional deformation accommodated by EW strike-slips during a regional transpressional phase.

The NW area of Tunisia is characterized by lateral and in-depth variations of facies, unconformities, sedimentary gaps, and folded and faulted structures. Such structures are interpreted as Neogene-Quaternary thrusting forming a fold-fault at subsurface beneath well W6. To explain the accommodation of the deformation within Kalaa Khesba graben, a model was proposed by combining the various tectonic phases, the strike-slip and thrust faults at subsurface (Fig. 17). It resulted in complex structures appearing following several tectonic events (compressions and extensions). A fold-fault, occurring within well W6, shows the presence of reverse faults induced by Neogene-Quaternary thrusting (Figs. 16-17). The study area associated with a dextral strike-slip through a reactivation suggesting a main transpressional constraint σ_1 oriented N160°. The opening of Kalaa Khesba Graben is generated as a pull-apart basin during Miocene. This stress regime generated NE-SW folds. From where one can conclude that these grabens of NW of Tunisia represent basins favorable for the fast accumulation of sediments which may contain organic matter.

Acknowledgements

We would like to express our sincere appreciations to the Entreprise Tunisienne d'Activités Pétrolières (ETAP), the Office National des Mines (ONM) and the Centre de Recherches et des Technologies des Eaux (CERTE) for providing Seismic and gravity data and scientific

support. We gratefully acknowledge the three anonymous reviewers who helped in improving the quality of this manuscript.

References

Barrier, E., Bouaziz, S., Angelier, J., Creuzot, J., Ouali, J., Tricart, P., 1993. Mesozoic paleostress evolution in the Saharan platform (Southern Tunisia). *Geodyn. Acta*, 6(1), 39-57.

Bejaoui, H., Aïfa, T., Melki, F., Zargouni, F., 2017. Structural evolution of Cenozoic basins in northeastern Tunisia, in response to sinistral strike-slip movement on the El Alia-Teboursouk Fault. *J. African Earth Sci.*, 134, 174-197.

Belguith, Y., Geoffroy, L., Rigane, A., Gourmelen, C., Ben Dhia, H., 2011. Neogene extensional deformation and related stress regimes in central Tunisia. *Tectonophysics*, 509, 198-207.

Belghithi, H., Boulvain, F., Yaich, C., Da Silva, A.C., 2016. Evolution des séries silicoclastiques miocènes en Tunisie centrale : Cas de la coupe de Khechem El Artsouma. *Carnets Geol., Madrid*, 16 (23), 557-568.

Ben Ayed, N., 1986. Evolution tectonique de l'avant pays de la chaine alpine de la Tunisie du début du Mésozoïque à l'actuel. *Thèse d'Etat*, Univ. Paris XI, 327p.

Ben Chelbi, M., Melki, F., Zargouni, F., 2006. Mode de mise en place des corps salifères dans l'Atlas septentrional de Tunisie. Exemple de l'appareil de Bir Afou. *C.R. Geoscience*, 338, 349-358.

Ben Jemiaa, M., 1986. Evolution tectonique de la zone de failles Trozza-Labeïed (Tunisie centrale). *Thèse 3ème Cycle*, Univ. Paris Sud Orsay, France, 158p.

Ben Romdhane, M., Brahim, N., Ouali, J., Mercier, E., 2006. Tectonique quaternaire et plis de rampe dans le golfe d'Hammamet (offshore tunisien). *Comptes Rendus Geoscience*, 338(5), 341-348.

Blakely, R.J., Simpson, R.W., 1986. Approximating edges of source bodies from magnetic or gravity anomalies. *Geophysics*, 51(7), 1494-1498.

Bouaziz, S., Barrier, E., Angelier, J., Turki, M.M., 1994. Paleostress in the Southern Tunisian platform. In: Roure, F. (Ed.), Peri-Tethyan Platforms. *Technip Editions*, France, 179-196.

Bouaziz, S., 1995. Etude de la tectonique cassante dans la plateforme et l'Atlas saharien (Tunisie méridionale): évolution des paléochamps de contraintes et implications géodynamiques. *Thèse Doc. Etat*, Univ. Tunis II, Tunisia, 485p.

Bouaziz, S., Barrier, E., Angelier, J., Tricart, P., Turki, M.M., 1998. Tectonic evolution of Southern Tethyan margin in southern Tunisia. In: Crasquin-Soleau, S., Barrier, E. (Eds.), Peri-Tethys Memoir: 3. Stratigraphy and Evolution of Peri-Tethyan Platforms, 177. *Mem. Mus. Natl. Hist. Nat*., Paris, 215-236.

Bouaziz, S., Barrier, E., Soussi, M., Turki, M.M., Zouari, H., 2002. Tectonic evolution of the northern African margin in Tunisia from paleostress data and sedimentary record. *Tectonophysics*, 357, 227-253.

Bouillin J.P., 1986. Le « bassin maghrébin » : une ancienne limite entre l'Europe et l'Afrique à l'ouest des Alpes. *Bull. Soc. géol. France*, 8(2), 547-558.

Burollet, P.F., 1956. Contribution à l'étude stratigraphique de la Tunisie centrale. *Annales des Mines et de la Géologie*, Tunis, vol.18, 350p.

Burollet, P.F., Rouvier, H., 1971. La Tunisie. *Unesco, Tectonique de l'Afrique* (Sciences de la Terre), 6, 600p.

Burollet, P.F., 1991. Structures and tectonics of Tunisia. Elsevier Science Publishers B.V, Amsterdam. *Tectonophysics*, 195, 359-369.

Caire, A., 1971. Chaînes alpines de la Méditerranée centrale (Algérie et Tunisie septentrionales, Sicile, Calabre et Apennin méridional). *Unesco, Tectonique de l'Afrique* (Sciences de la Terre, 6), 584p.

Castany, G., 1952. Paléogéographie, tectonique et orogénèse de la Tunisie. *Congrès géologique international*, 1, 63p.

Chihi, L., 1995. Les fossés néogènes à quaternaires de la Tunisie et de la mer pélagienne : Leur étude structurale et leur signification dans le cadre géodynamique de la Méditerranée centrale. *Thèse de Doctorat d'Etat*, Faculté des Sciences Tunis, 385p.

Chihi, L., Ben Haj Ali, M., Ben Ayed, N., 1992. Mécanismes et signification structurale du plissement dans les chaînes des Chotts (Tunisie méridionales). Analogie avec les plis associés au décrochement E-W de Sbiba (Tunisie Centrale). *C. R. Acad. Sci.*, Paris, t.315, série II, 1245-1252.

Chikhaoui, M., Jallouli, C., Turki, M.M., Soussi, M., Braham, A., Zaghbib-Turki, D., 2002. L'affleurement triasique du Debadib-Ben Gasseur (Nord-Ouest de la Tunisie) : diapir enraciné à épanchements latéraux dans la mer Albienne, replissé au cours des phases de compression tertiaires. *C.R. Géoscience*, 334(16), 1129-1133.

Delteil, J., Zouari, H., Chikhaoui, M., Creuzot, G., Ouali, J., Turki, M.M., Yaich, C., Zargouni, F., 1991. Relation entre ouvertures téthysiennes et mésogeénnes en Tunisie. *Bull. Soc. Geol. France*, 162(6), 1173-1181.

Dlala, M., 1996. La tectonique cénozoïque du Nord de la Tunisie dans son contexte de de collision-subduction. *Proceedings of the 5th Tunisian Petroleum Conference, Tunis, Tunisia. ETAP Memoir*, 10, 337-346.

Dlala, M., 2001. Les manifestations tectono-sédimentaires d'âge Campanien–Maastrichtien en Tunisie: implications sur l'évolution géodynamique de la marge Nord-Africaine. *C.R. Geoscience*, 334, 135-140.

El Euchi, H., Fourati, L., Hamouda, F., Saidi, M., 1998. Structural style and hydrocarbon habitat in Northern Tunisia. *Field Trip Guide Book. ETAP Memoir*, 13, Tunis, Tunisia, 72p.

Ezzine, I., Ghanmi, M., Ben Youssef, M., Zargouni, F., 2008. Modèle du pli de propagation de rampe : exemple Jebel Bou El Hanèche. *22nd colloquium of African Geology*, Nov. 4-6, Hammamet, Tunisia, p.341.

Ezzine, I., 2011. Apport des données satellitaires et gravimétriques à l'étude géologique de la région de Maktar-Tadjerouine (Tunisie Centro-Septentrionale). *Thèse de Doctorat*, Université Tunis El Manar, Tunis, 294p.

Ezzine, I., Jaffal, M., Ben Youssef, M., Zargouni, F., Ghanmi, M., 2012. The thrust front in the Jebel Bou El Hanèche - Kalâat Khasba (Central-northern Tunisia). Integration of geological and geophysical data. *Estudios Geológicos*, 68(2), 165-177, doi:10.3989/egeol.40378.128.

Gabtni, H., Gouasmia, M., 2013. Joint evaluation of gravity, electrical and magnetotelluric methods for geothermal potential of fractured Aptian reefal carbonates in the Hmaima-El Gara area (Oued Serrat basin, Central-Western Tunisia). *J. Afr. Earth Sci.*, 6, 1569-1579.

Gabtni, H., Hajji, O., Jallouli,C., 2016. Integrated application of gravity and seismic methods for determining the dip angle of a fault plane: Case of Mahjouba fault (Central Tunisian Atlas Province, North Africa). *J. Afr. Earth Sci.*, 119, 160-170.

Gabtni, H., Jallouli, C., 2017. Regional-residual separation of potential field: An example from Tunisia. *J. Appl. Geophy.*, 137, 8-24.

Geosoft incorporated, 2013. Software for earth science mapping and processing [Oasis Montaj]. *Geosoft Inc. Ltd.*: www.geosoft.com

Ghanmi, M., Vila, J.M., Ben Youssef, M., Bouhlel, S., Zargouni, F., 2001. Vers l'abondon du modèle de diapir en champignon anté-vranconien au Jebel Slata : Découverte sur son flanc NW d'Albien inférieur et d'Albien moyen, à leur place dans une série à l'endroit. *Notes du Serv. géol. Tunisie*, 68, 59p.

Ghanmi, M., 2003. Géodynamique de la plateforme saharienne et sa marge septentrionale au Crétacé, son évolution vers l'Atlas septentrional, interférences du rifting et de l'halocinèse. *Habilitation à diriger des recherches*, Université Tunis El Mannar II, 347p.

Hennebert, M, Dupuis, C., 2003. Use of cyclostratigraphy to build a high-resolution time-scale encompassing the Cretaceous-Palaeogene boundary in the Aïn Settara section (Kalaat Senan, Central Tunisia). *Geobios*, 36, 707-718.

Inoubli, N., Gouasmia, M., Gasmi, M., Mhamdi, A., Ben Dhia, H., 2006. Integration of geological, hydrochemical and geophysical methods for prospecting thermal water resources: The case of the Hmeïma region (Centre-Western Tunisia). *J. Afr. Earth Sci.*, 46, 180-186.

International Association of Geodesy, 1971. Geodetic Reference System 1967, numéro 3, spec. publ. *Bureau Central de l'Association Internationale de géodésie*, 116p.

Jacobsen, H., 1987. A case for upward continuation as a standard separation filter for potential-field maps. *Geophysics*, 52(8), 1138-1148.

Kingdom software, 2015. SMT/IHS version 9.0 Advanced: www.ihs.com/kingdom

Lehotsky, I., Bujnowsky, A., 1995. Notice explicative : carte géologique de Kalat Es Senan. Feuille n°59.

Martinez, C., Truillet, R. 1987. Evolution structurale et paléogéographie de la Tunisie. *Memoria de la Societa Italiana de Geologia*, (38), 35-45.

Martinez, C., Chikhaoui, M., Truillet, R., Ouali, J., Greuzot, G., 1991. Le contexte géodynamique de la distension albo-aptienne en Tunisie septentrionale et centrale: structuration éocrétacée de l'Atlas tunisien. *Eclogae geol. Helv.*, 84(1), 61-82.

ONM, 1997. Campagne gravimétrique CG5. Coupures 1/50000 de Kalaat Senam et Tajerouine.

Pace, P., Calamita, F., 2014. Push-up inversion structures v. fault-bend reactivation anticlines along oblique thrust ramps: examples from the Apennines fold-and-thrust belt (Italy). *Journal of the Geological Society London*, 171, 227-238.

Perthuisot, V., Rouvier, H., Smati, A., 1988. Style et importance des déformations anté-vraconiennes dans le Maghreb sriental: exemple du diapir du Jebel Slata (Tunisie centrale). *Bull. Soc. géol. France*, 8, IV(3), 391-398.

Perthuisot, V., Aoudjehane, M., Bouzenoune, A., Hatira,N., Laatar, E., Mansouri, A., Rouvier, H., Smati, A., Thibieroz, J., 1998. Les Corps triasiques des monts du Mellégue (confins algéro-tunisiens) sont-ils des diapirs ou des glaciers de sel. *Bull. Soc. géol. France*, 169(1), 53-61.

Pervinquière, L., 1903. Etude géologique de la Tunisie centrale. *Doct. ès. Sci.*, Paris, 360p.

Reid, A.B., Allsop, J.M., Granser, H., Millet, A.J., Somerton, I.W., 1990. Magnetic interpretation in three dimensions using Euler deconvolution. *Geophysics*, 55 (1), 80-91.

Richert, J.P., 1971. Mise en évidence de quatre phases tectoniques successives en Tunisie. *Not. Serv. Géol. de Tunisie*, 34, Tunis, 115-125.

Robaszynski, F., Maria, J., Donoso, G., Linares, D., Amédro, F., Caron, M., Dupuis, C., Dhondt, A., Gartner, S., 1998. Le Crétacé supérieur de la région de Kalat Es Senan, Tunisie centrale. Lithostratigraphie intégrée: zones d'ammonites, de foraminifères planctoniques et de nannofossiles du Turonien supérieur au Maastrichtien. *Bull. Centre Recherche Elf Explor. Prod.*, 22(2), 359-490.

Rosenbaum, G., Lister, G.S., Duboz, C., 2002. Reconstruction of the tectonic evolution of the western Mediterranean since the Oligocene. *J. Virt. Expl.*, 8, 107-126.

Roure, F., Casero, p., Addoum, B., 2012. Alpine inversion of the North African margin and delamination of its continental lithosphere. *Tectonics*, 31, TC3006, doi:10.1029/2011TC002989.

Smati, A., 1983. Approche géologique et minière de la partie méridionale du massif du Slata (Tunisie du centre nord). *Rapport de DEA*, 350p.

Soumaya, A., Ben Ayed, N., Delvaux, D., Ghanmi, M., 2015. Spatial variation of present-day stress field and tectonic regime in Tunisia and surroundings from formal inversion of focal mechanisms: Geodynamic implications for central Mediterranean. *Tectonics*, 34, 1154-1180, doi:10.1002/2015TC003895

Spector, A., Grant, F.S., 1970. Statistical models for interpreting aeromagnetic data. *Geophysics*, 35, 293-302.

Turki, M.M., Delteil, J., Trullet, R., Yaich, C., 1988. Les inversions tectoniques de la Tunisie centro-septentrionale. *Bull. Soc. géol. France* (8), I-IV(3), 399-406.

Thompson, D. T., 1982. EULDPH : A new technique for making computer-assisted depth estimates from magnetic data. *Geophysics*, 47, 31-37.

Yaich, C., 1984. Etude géologique des chaïnons de Chérahil et du Krechem el Artsouma (Tunisie centrale). Liaison avec les structures profondes des plaines adjacentes. *Thèse 3ème Cycle*, Univ. Besançon, France, 165p.

Zargouni, F., 1984. Style et chronologie des déformations des structures de l'Atlas tunisien méridional. *C.R. Acad. Sc.*, Paris, 299, série II(2), 71-76.

Zargouni, F., 2011. La mégastructure anticlinale de Semda (Sraa Ouartane). *Rapport interne*, 31 juin, Oil Search (Tunisia) Ltd., 17p.

Zouari, H., 1995. Evolution géodynamique de l'Atlas centro-méridional de la Tunisie: Stratigraphie, analyse géométrique, cinématique et tectono-sédimentaire. *Thèse Doc. Etat*, Univ. Tunis II, Tunisia, 278 p.

Table captions

Table 1: Detailed description of the lithostratigraphic column of well W6.

Table 2: Wells W1-W6 identity card. TD: total depth.

Figure captions

Fig. 1: (a) Structural map of Tunisia, rectangle: Location of the study area (northwestern Tunisia). **(b)** Simplified geological map of the study area extracted from the map of Tunisia at 1/50,000, projected on a WGS84 UTM Z32 N system. 1. Quaternary, 2. Mio-Pliocene, 3. Upper Miocene, 4. Oligocene, 5. Ypresian-Lutetian, 6. Coniacian-Maastrichtian, 7. Turonian, 8. Cenomanian, 9. Early Cretaceous, 10. Triassic.

Fig. 2: **(a)** Lithostratigraphic correlation between wells W1 to W4 (see Fig. 1b for the location of wells). **(b)** Lithostratigraphic correlation of wells W5, W3 and W6. Same notations as in Fig. 2a.

Fig. 3: Map showing locations of all seismic lines in the NW study area of Tunisia. W1-W6: Oil wells, L1-L3: seismic lines interpreted.

Fig. 4: (a) SW-NE oriented seismic line L1 across the graben. **(b)** Traces of major faults and the various horizons, namely the tops of the following units: 1. Segui , 2. O. Bel Khedim, 3. Oum Dhouil, 4. Cherahil, 5. El Gueria, 6. Chouabine, 7. El Haria, 8. Abiod, 9. Bireno, 10. Serdj, 11. Triassic evaporates. **(c)** Interpretation of the seismic line L1: 12. Pliocene, 13. Middle-Late Miocene, 14. Lower Eocene-Paleocene, 15. Upper Cretaceous, 16. Lower Cretaceous, 17. Late Triassic. W6: exploration well, TWT (s): Two way time (s).

Fig. 5: (a) SW-NE oriented seismic line L2 across the graben. **(b)** Traces of major faults and the various horizons. **(c)** Interpretation of the seismic line L2. Same notations as in Fig. 4.

Fig. 6: (a) SW-NE and NW-SE oriented composite seismic line L3 (L1+L2) across the graben. **(b)** Traces of major faults and the various horizons. **(c)** Interpretation of the composite seismic line L3. Same notations as in Fig. 4.

Fig. 7: Isochron map at the top of Serdj formation, showing three types of ways of dip closure: 1. Semda; 2. Mahjouba; 3. Thala. Isocontours and colours are given in TWT (s).

Fig. 8: Isovelocity map at the top of Serdj formation. Isocontours and colours are given in m/s.

Fig. 9: Isobath map at the top of Serdj formation, showing the main faults oriented NW-SE to NS and NE-SW to EW. Isocontours and colours are given in meters.

Fig. 10: Bouguer Anomaly map of Kalaa Khesba and Kalaat Senam computed using a density value of 2.4 $g.cm^{-3}$, projected on a WGS84 UTM Z32 N system. 1: Dj. Jerissa, 2: Dj. Bou Afna.

Fig. 11: Regional map of order 3 of Kalaa Khesba and Kalaat Senam.

Fig. 12: Residual map of order 3 of Kalaa Khesba and Kalaat Senam.

Fig. 13: Energy radial spectrum of Bouguer gravity field vs. frequency unit in cycles/km of Kalaa Khesba, Kalaat Senam. Depths are given by the slope values. 1. $z_1 = 3.2$ km, 2. $z_2 = 1.65$ km, 3. $z_3 = 0.8$ km.

Fig. 14: Horizontal gravity gradient (HGG) map of Kalaa Khesba and Kalaat Senam in mGal/m indicating the main structural features with their dips.

Fig. 15: Euler Deconvolution map for Euler Solutions (depth in m) of Kalaa Khesba and Kalaat Senam.

Fig. 16: Push-up inversion structure above well W6 (see Table 1 for the lithology). The duplicated horizon (orange) is composed of El Haria, Chouabine and El Gueria Formations (Paleocene-Eocene).

Fig. 17: (a) Theoretical model for pull-apart basins initiation through transpressional regime. **(b)** Proposed model of Kalaa Khesba Graben showing a fold thrust and indicating the relationship between constrain σ_1, N160° oriented, and strike-slip and thrust faults. Note that the El Haria, Chouabine and El Gueria Formations (yellow), dated from Danian to Ypresian, are deformed and cross-cut by multiple faults (network faulting system F1-F9).

Well	Operator	Year	TD	TD@formation	Objective
W1	Aquitaine Tunisie	1970	957	Serdj	Petroleum exploration of the reservoirs of Serdj Formation providing indications or accumulations of hydrocarbons in the drillings.
W2	Total Exploration Tunisie	1981	2298.5	Serdj	Recognition of the carbonated facies which may contain good reservoirs and whose clayey side equivalent northwards constitutes the potential source rock.
W3	CGG Services	2011	3701	M'Cherga	The main targets are: * Dolomites of the Serdj Formation * Sandstone of Sidi Aich Formation
W4	Société nord-Africaine des Pétroles	1954	6601	Fahdene	Evolution of the northern part of Thala block (north of well W4). Stratigraphic objective: Serdj Formation, known through limestones and dolomites.
W5	Equipement Hydraulique	1967	1119.6	Fahdene	Stratigraphic and oil recognition of the Albian-Aptian series of the west Rohia anticline (SE Kalaa Khesba Graben).
W6	Mosbacher Tunisia LLC	1996	2064	Aleg	- Chouabine Formation - Nummulite of El Gueria Formation - Facies chalk of Abiod Formation

Chronostratigraphy	Formations	Depth (m)	Lithology	Description
Gelacian	Segui	10 307		sand, clay and conglomerat
Tortonian-Messinian	Oued Bel Khedim	390		
Langhian-Serravalian	Oum Dhouil			gypsum, sand and clay sandy clays
Lutetian	Cherahil	1200	F	alternance clay dolomite and marl
Tortonian-Messinian	Oum Dhouil	1240	F	sandy clays
Lutetian	El Gueria	1350		limestone
Ypresian	Chouabine	1390	F	alternance clay dolomite and marl
Danian	El Haria	1420		marl
Ypresian	Chouabine	1510		alternance clay dolomite and marl
Lutetian	El Gueria	1570		marl
Ypresian	Chouabine			alternance clay dolomite and marl
Lutetian	El Gueria	1580		limestone
Ypresian	Chouabine	1650		alternance clay dolomite and marl
Thanetian	El Haria	1800		marl
Campanian-Maastrichtian	Abiod	1900		limestone
Santonian-Campanian	Aleg	2000	F	marl with limestone levels
Turonian-Santonian	Trias	2064		gypsum and anhydrite

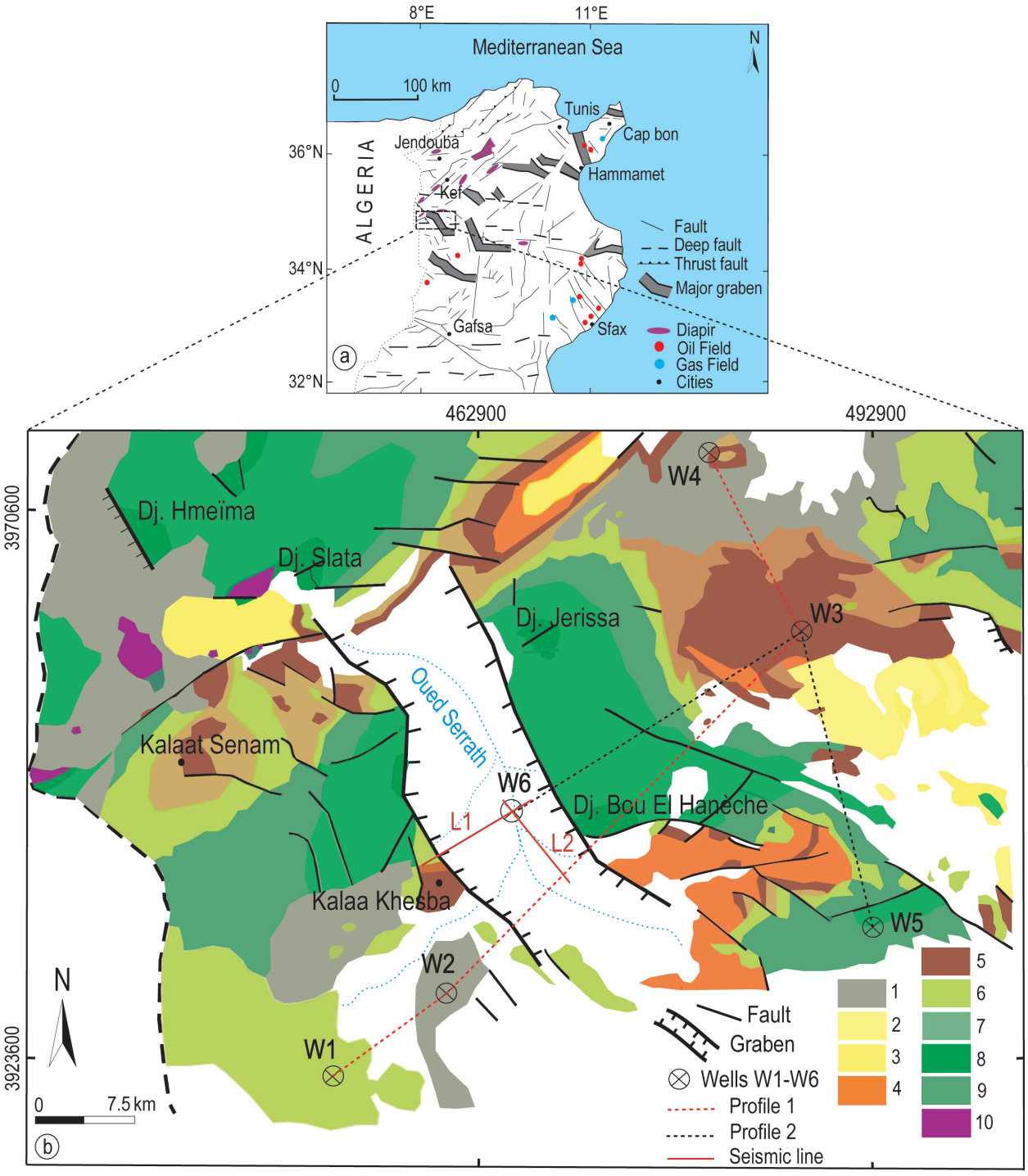
8°E
11°E
Mediterranean Sea
N
0
100 km
Tunis
Cap bon
Jendouba
36°N
ALGERIA
Hammamet
Kef
Fault
Deep fault
Thrust fault
Major graben
34°N
Gafsa
Sfax
Diapir
Oil Field
Gas Field
Cities
a
32°N
462900
492900
3970600
3923600
Dj. Hmeïma
Dj. Slata
W4
Dj. Jerissa
W3
Oued Serrath
Kalaat Senam
W6
L1
L2
Dj. Bou El Hanèche
Kalaa Khesba
W5
W2
W1
N
0
7.5 km
b
Fault
Graben
Wells W1-W6
Profile 1
Profile 2
Seismic line
1
2
3
4
5
6
7
8
9
10

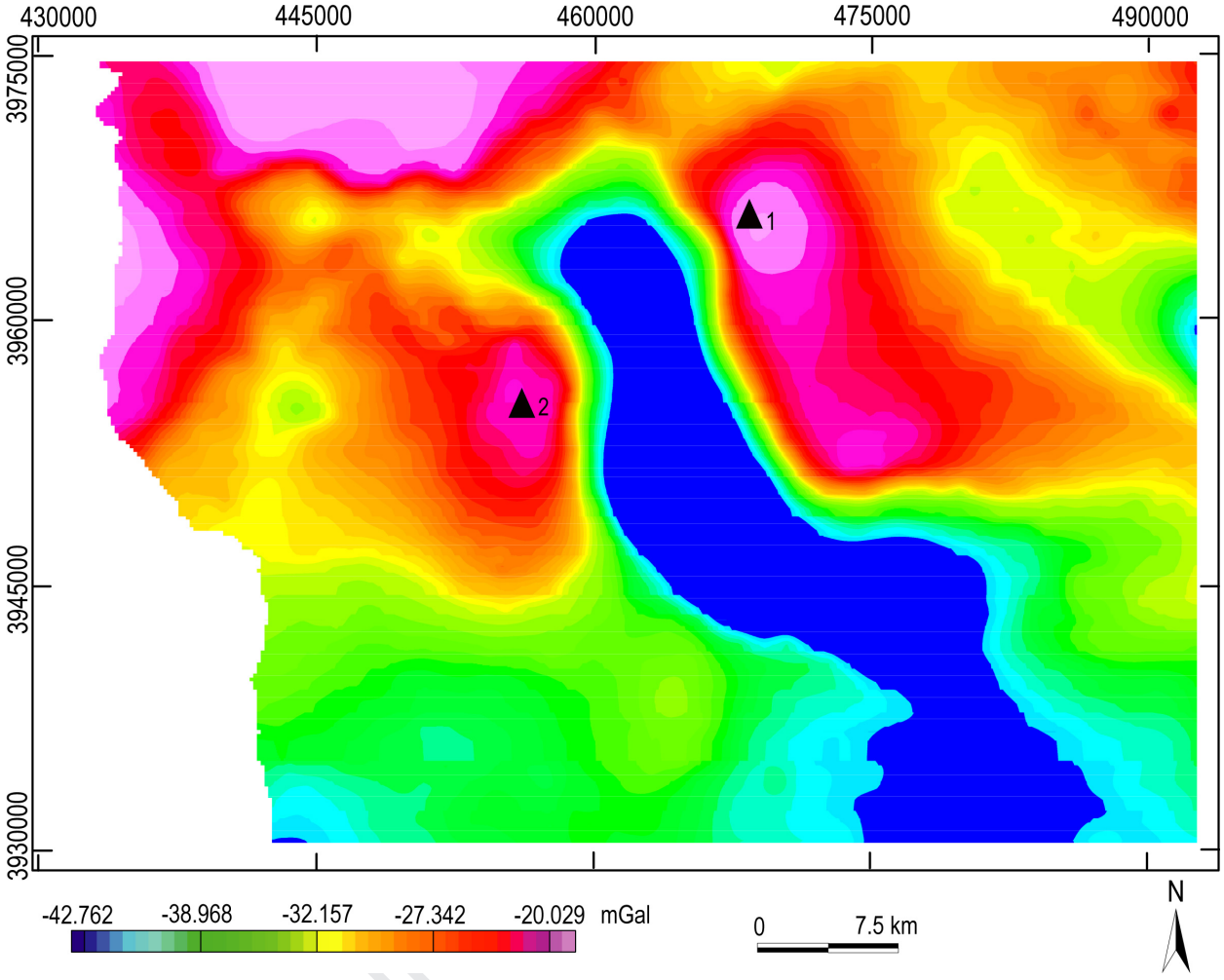
430000
445000
460000
475000
490000
3975000
3960000
3945000
3930000
1
2
-42.762
-38.968
-32.157
-27.342
-20.029
mGal
0
7.5 km
N

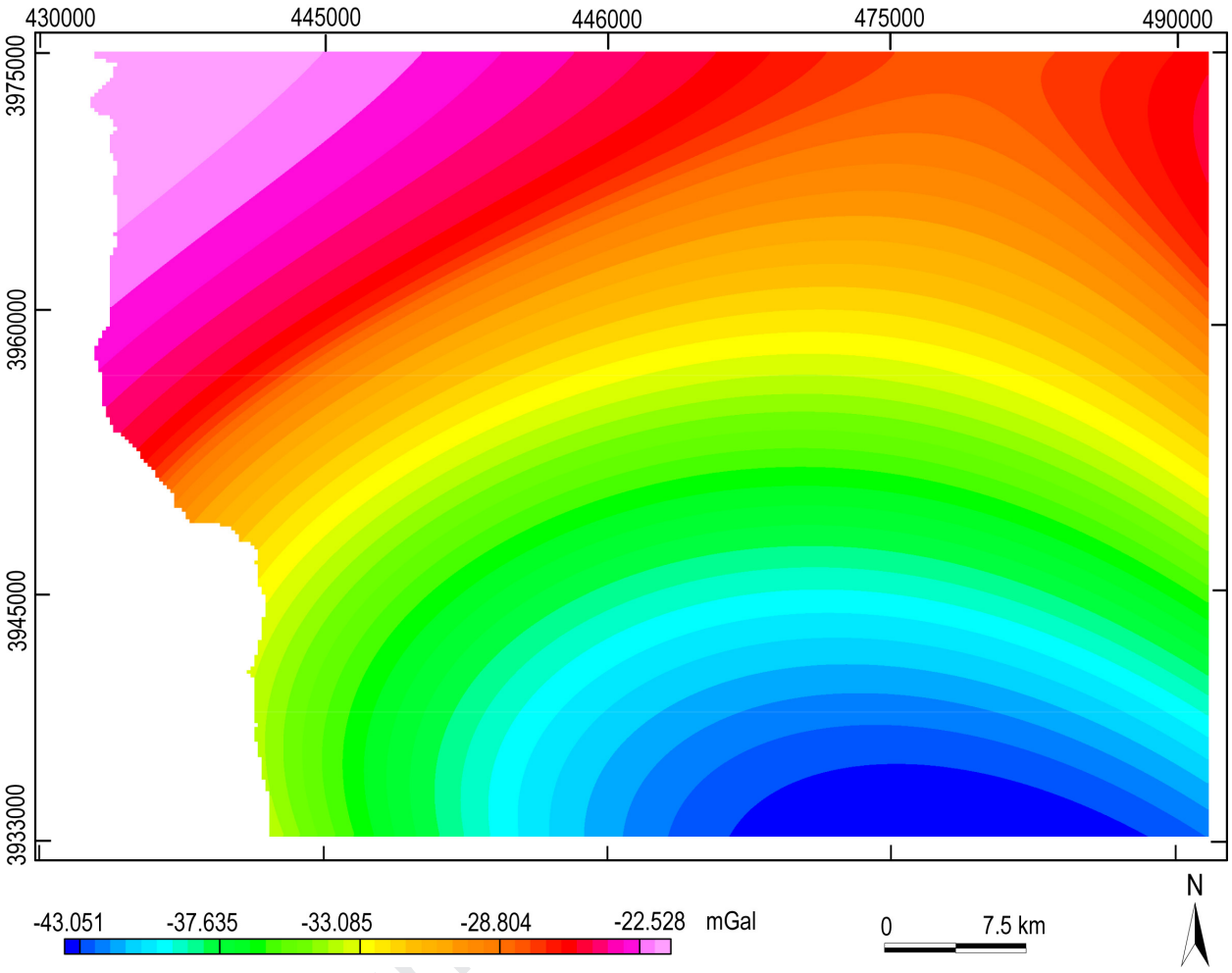

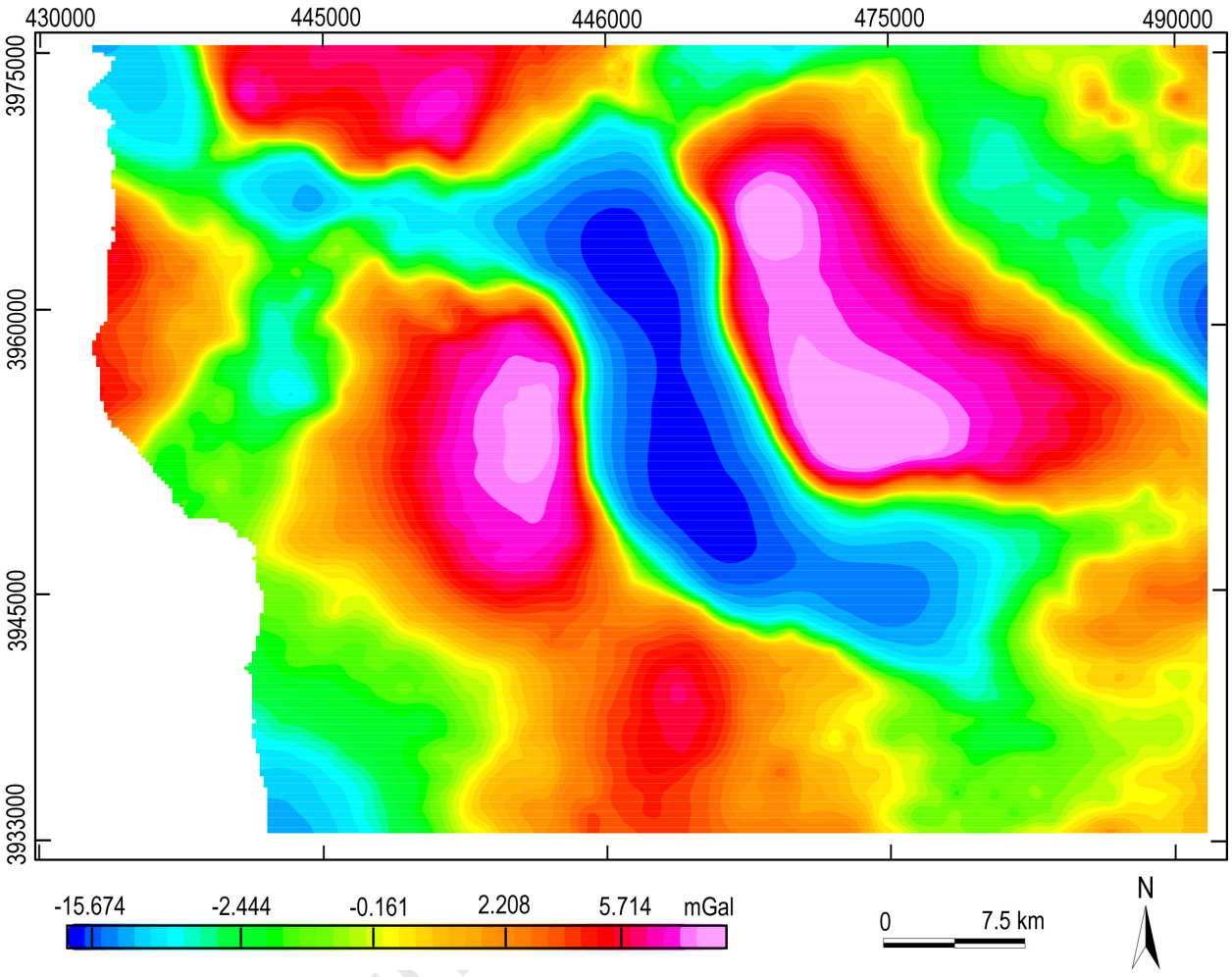

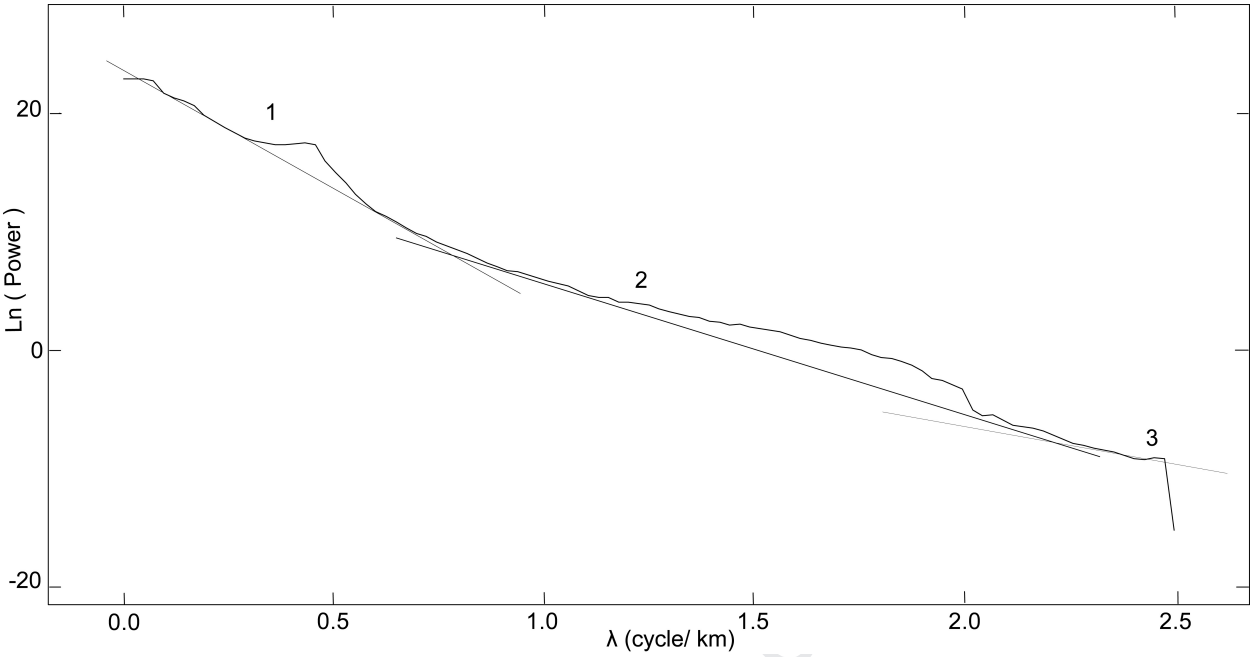

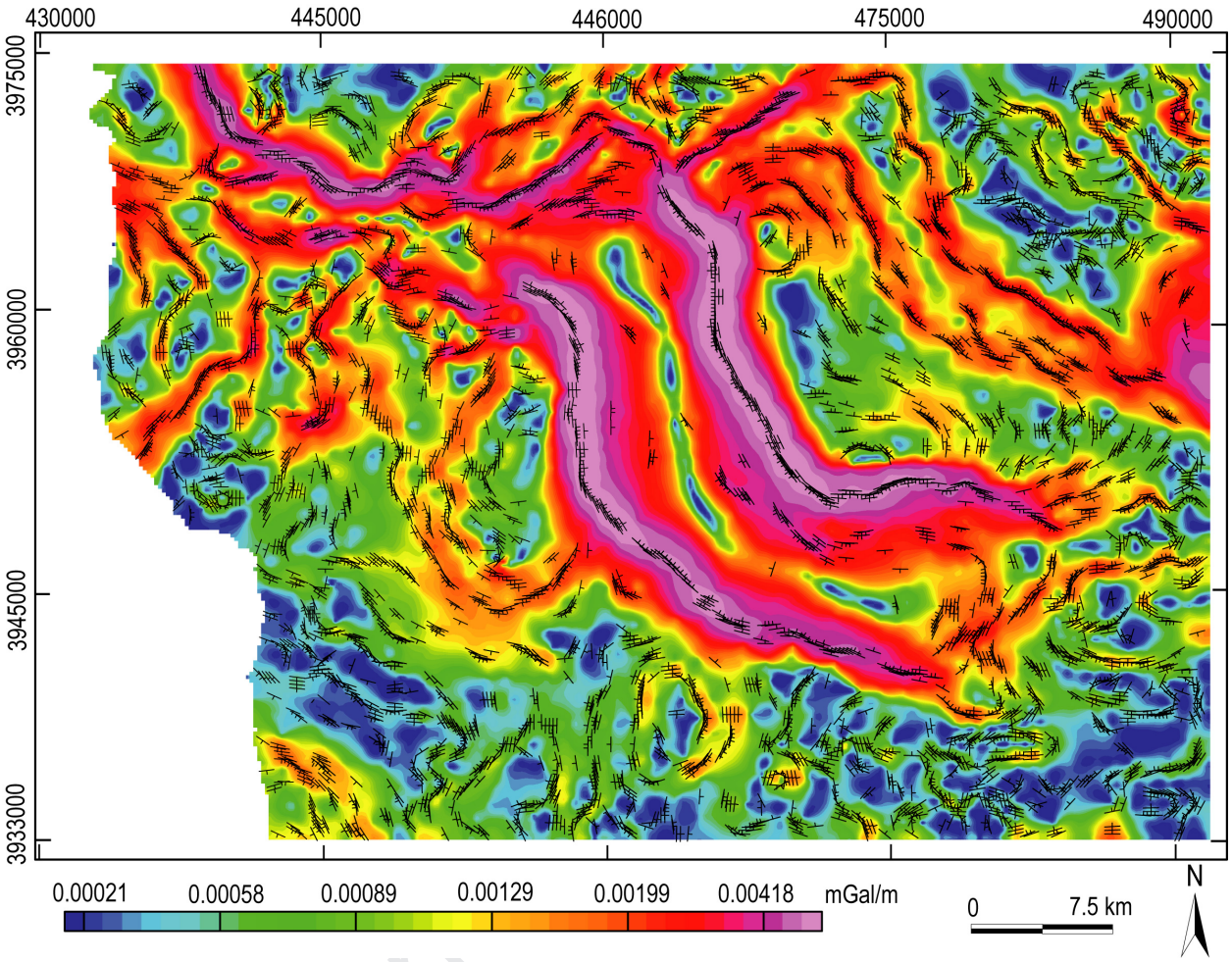

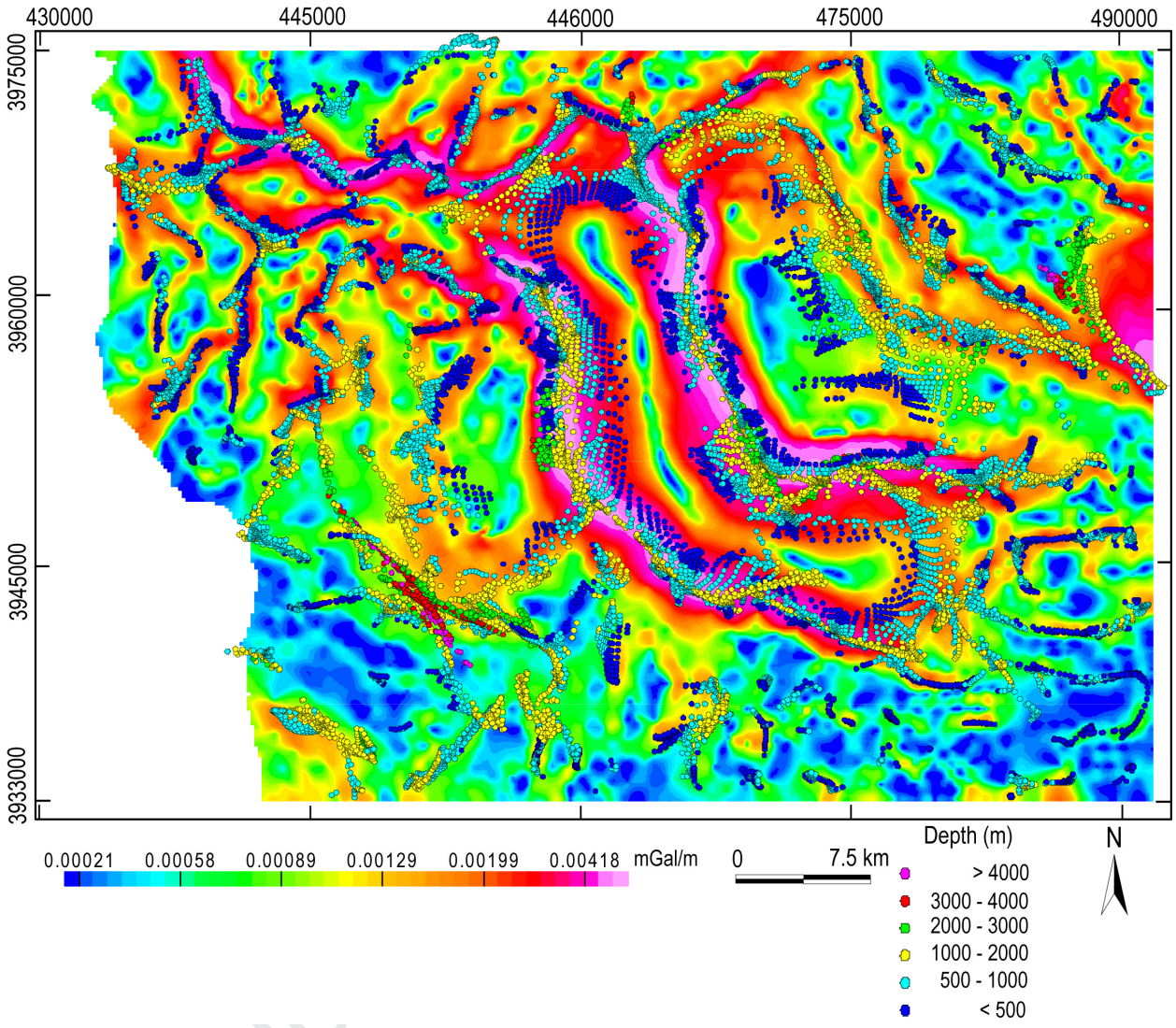
430000
445000
446000
475000
490000
3975000
3960000
3945000
3933000
0.00021
0.00058
0.00089
0.00129
0.00199
0.00418
mGal/m
0
7.5 km
Depth (m)
> 4000
3000 - 4000
2000 - 3000
1000 - 2000
500 - 1000
< 500
N

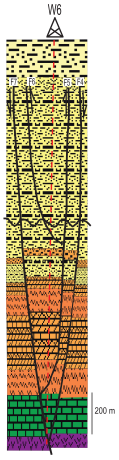

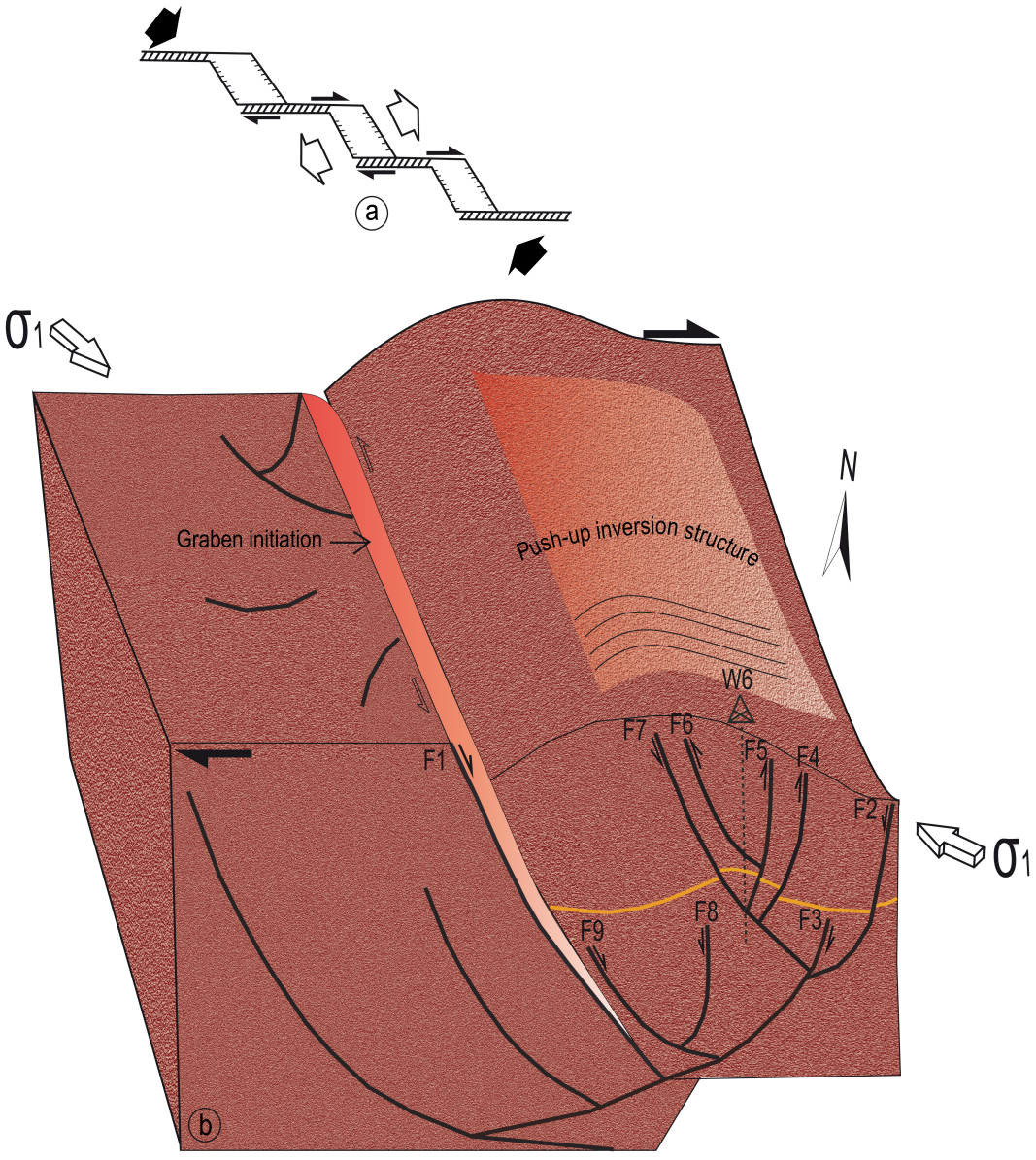
a
σ1
Graben initiation
Push-up inversion structure
N
W6
F7
F6
F5
F4
F2
F1
σ1
F8
F3
F9
b

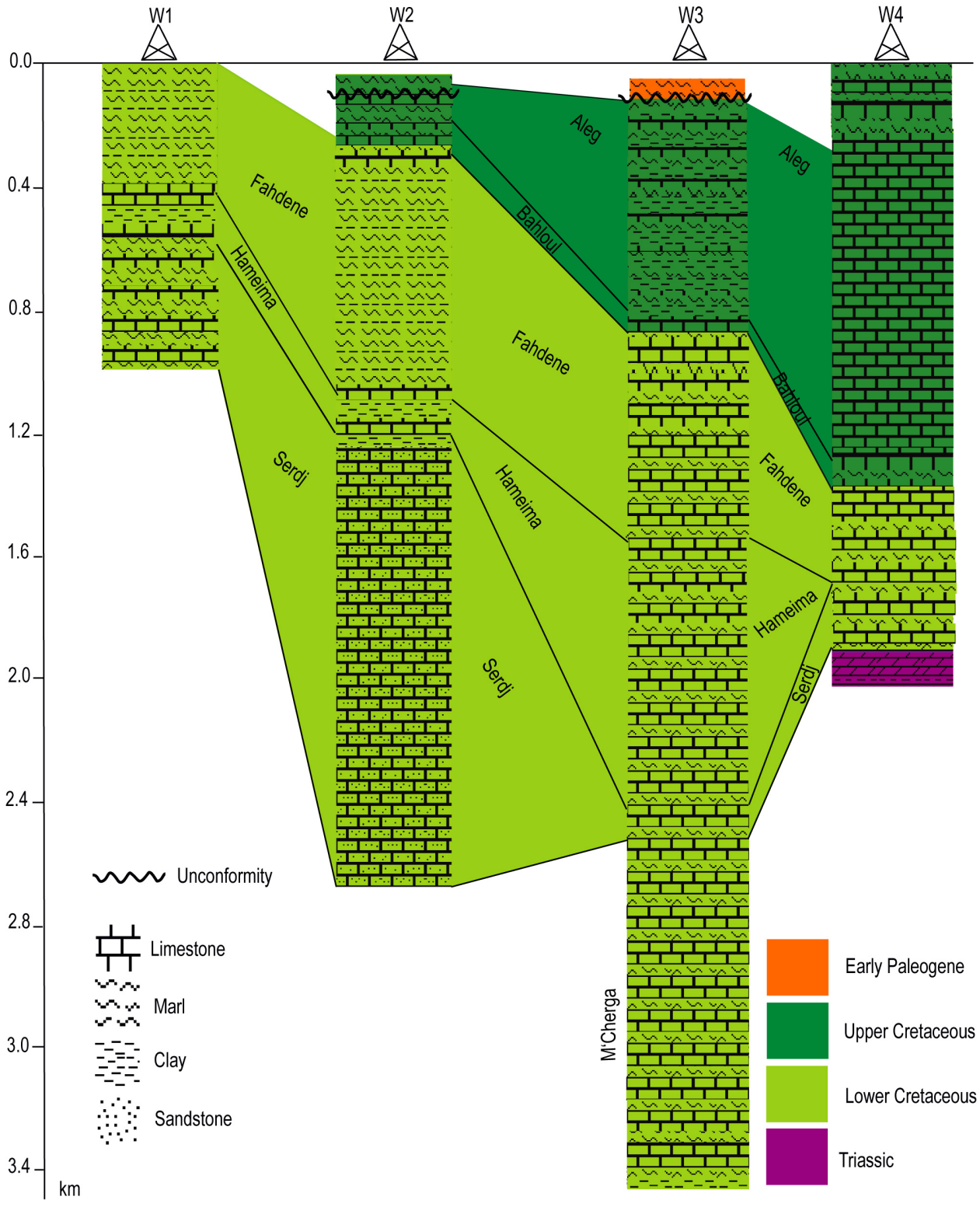
W1
W2
W3
W4
0.0
0.4
0.8
1.2
1.6
2.0
2.4
2.8
3.0
3.4
km
Fahdene
Hameima
Serdj
Aleg
Bahloul
Fahdene
Hameima
Serdj
Aleg
Bahloul
Fahdene
Hameima
Serdj
M'Cherga
Unconformity
Limestone
Marl
Clay
Sandstone
Early Paleogene
Upper Cretaceous
Lower Cretaceous
Triassic

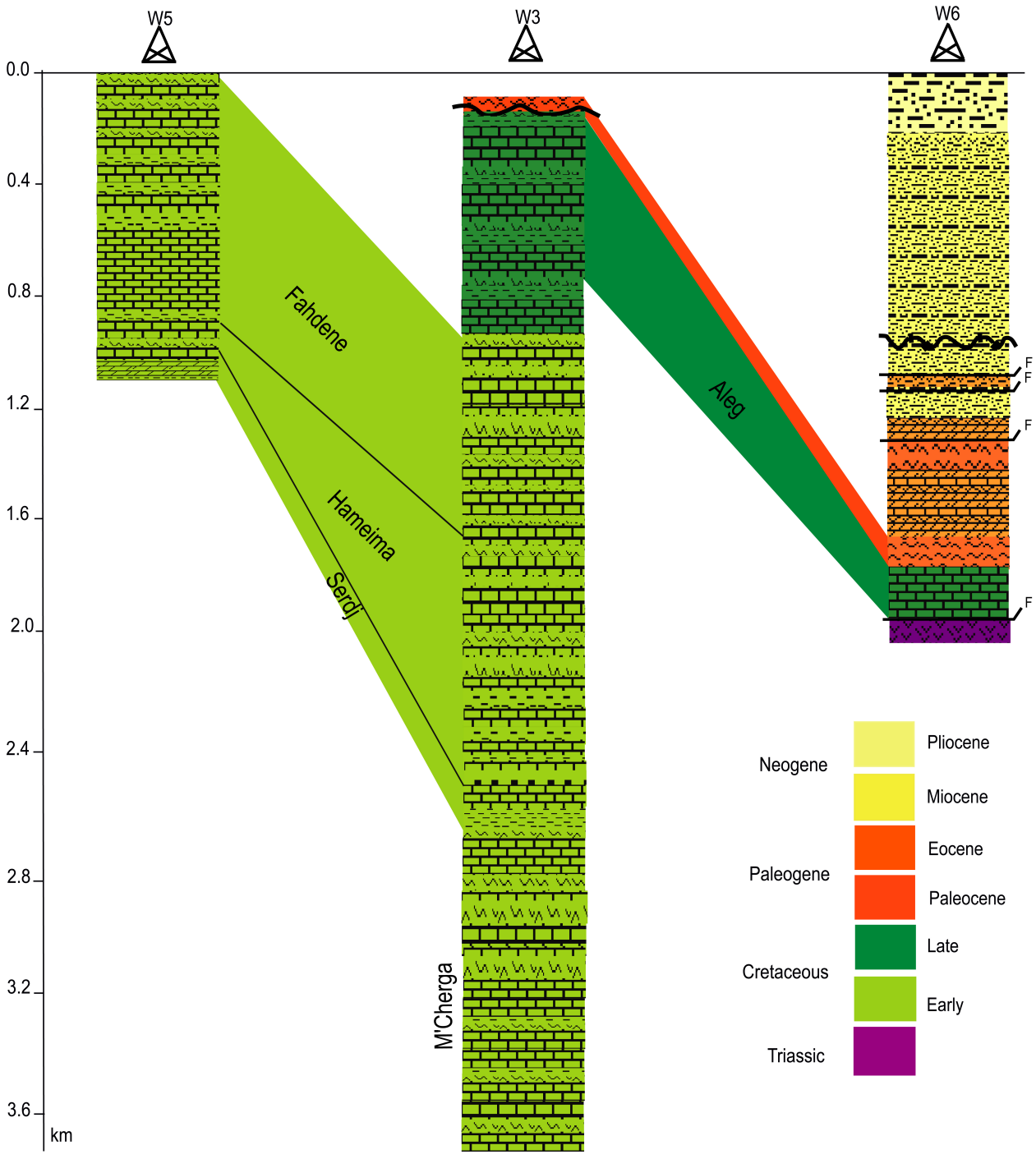
W5
W3
W6
0.0
0.4
0.8
1.2
1.6
2.0
2.4
2.8
3.2
3.6
km
Fahdene
Hameima
Serdj
M'Cherga
Aleg
F
F
F
F
Neogene
Pliocene
Miocene
Paleogene
Eocene
Paleocene
Cretaceous
Late
Early
Triassic

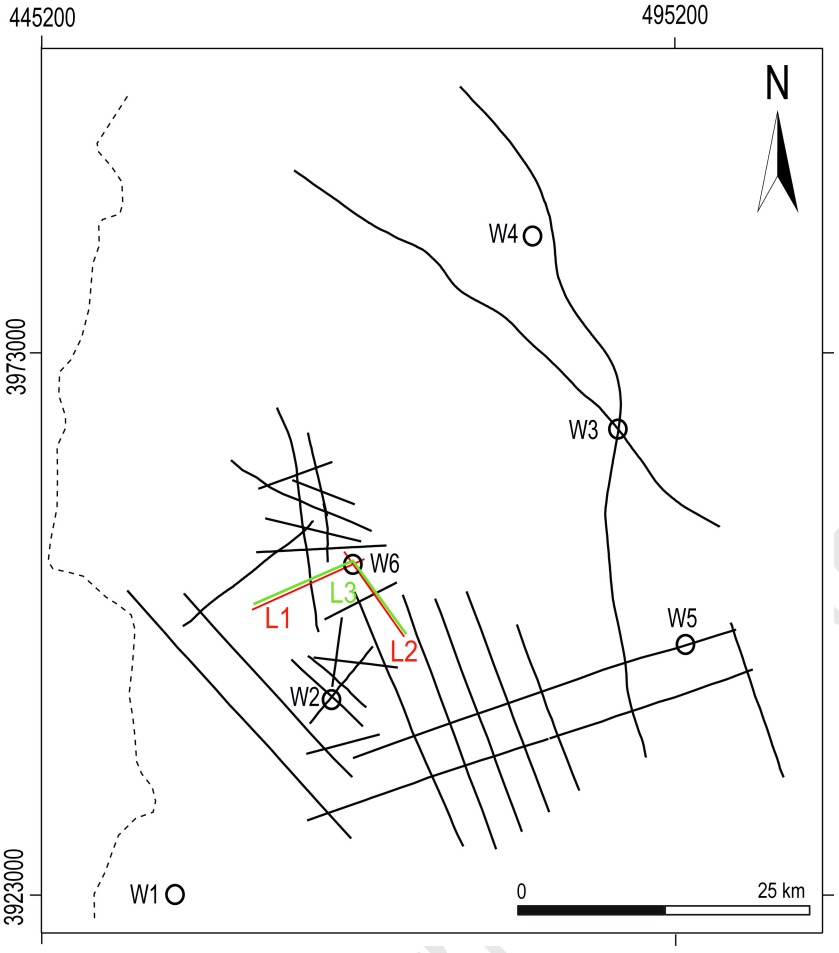

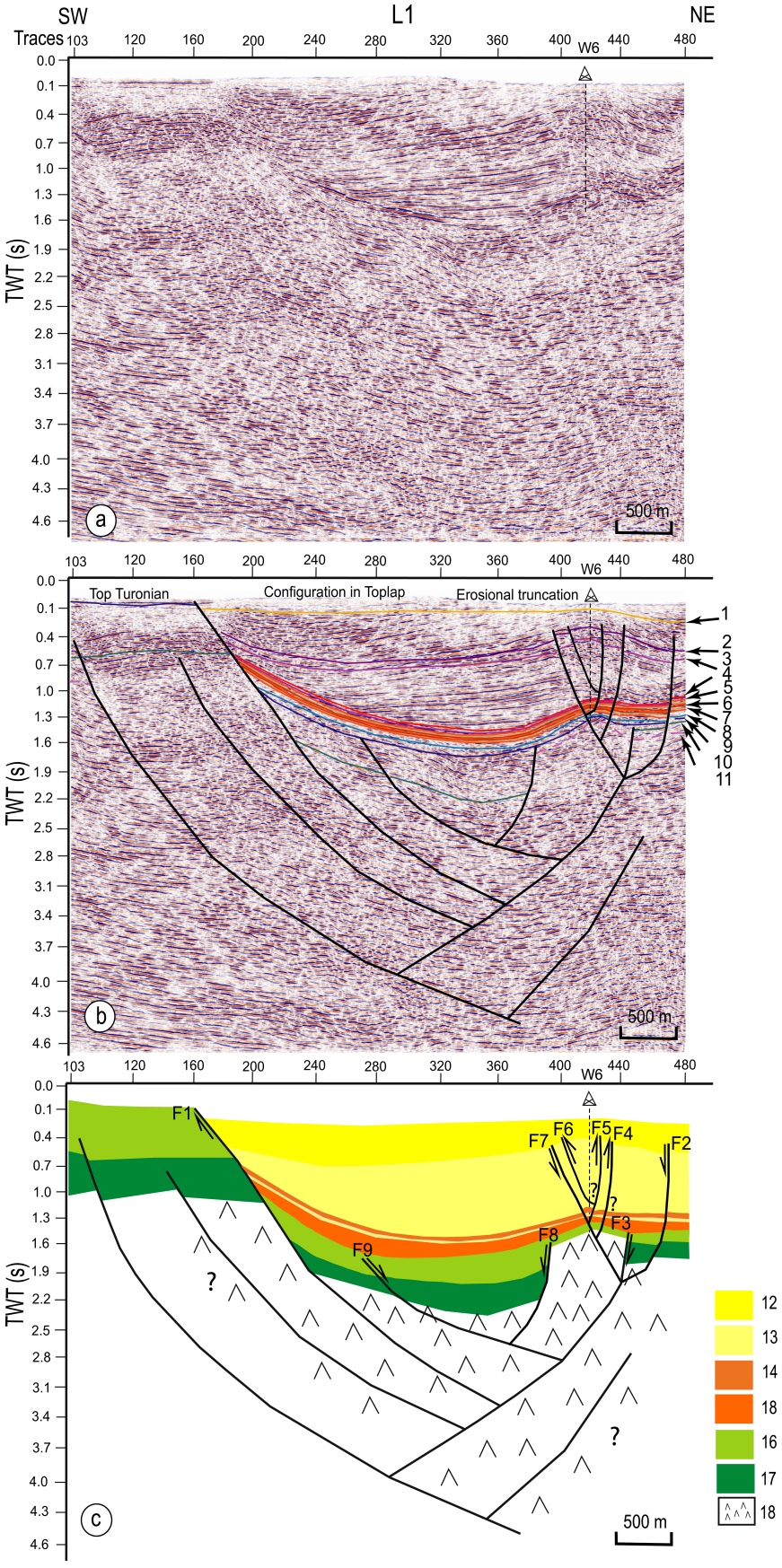

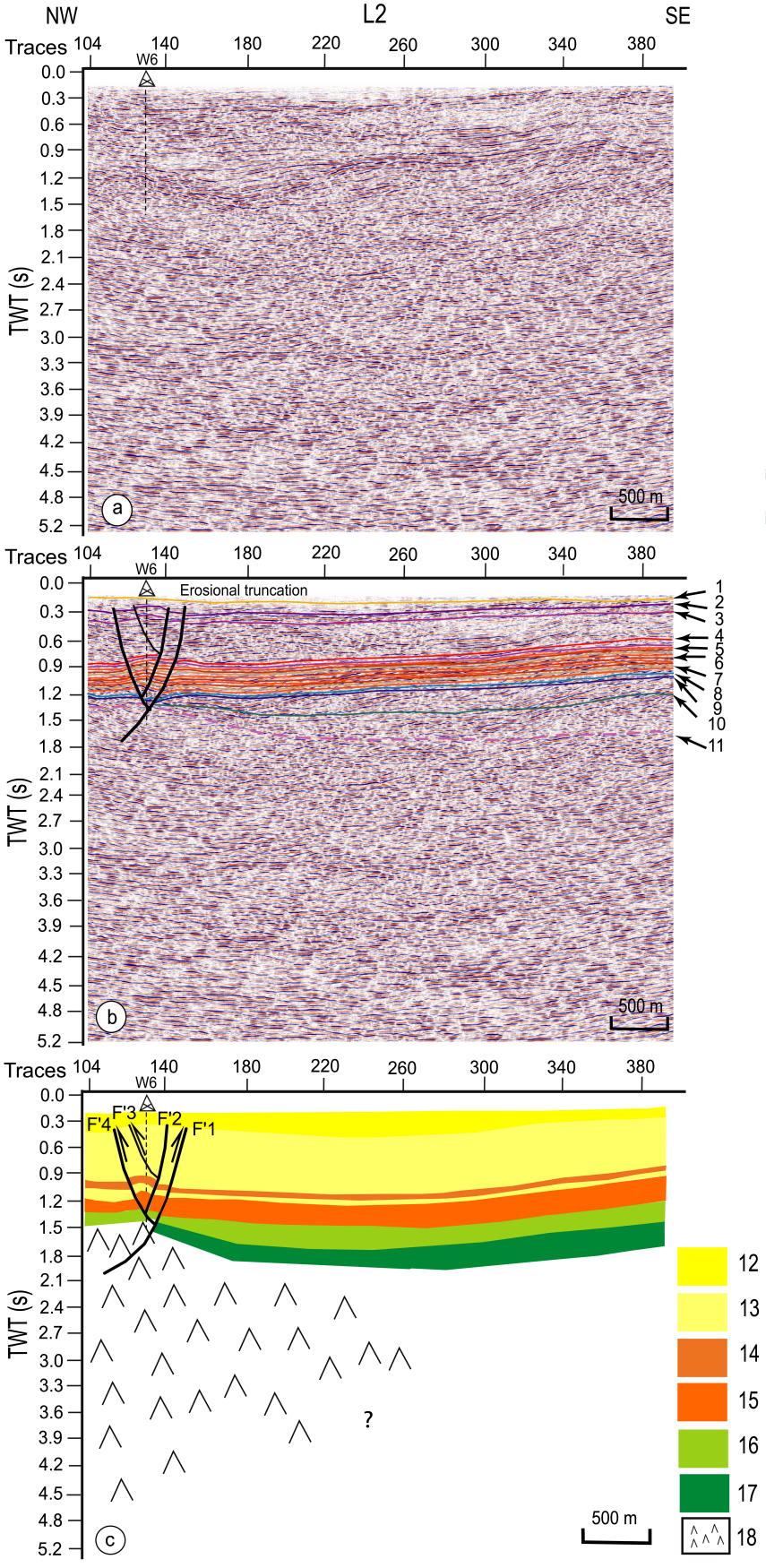
NW
L2
SE
Traces
104
140
180
220
260
300
340
380
W6
TWT (s)
0.0
0.3
0.6
0.9
1.2
1.5
1.8
2.1
2.4
2.7
3.0
3.3
3.6
3.9
4.2
4.5
4.8
5.2
a
500 m
Erosional truncation
1
2
3
4
5
6
7
8
9
10
11
b
F'4
F'3
F'2
F'1
?
12
13
14
15
16
17
18
c

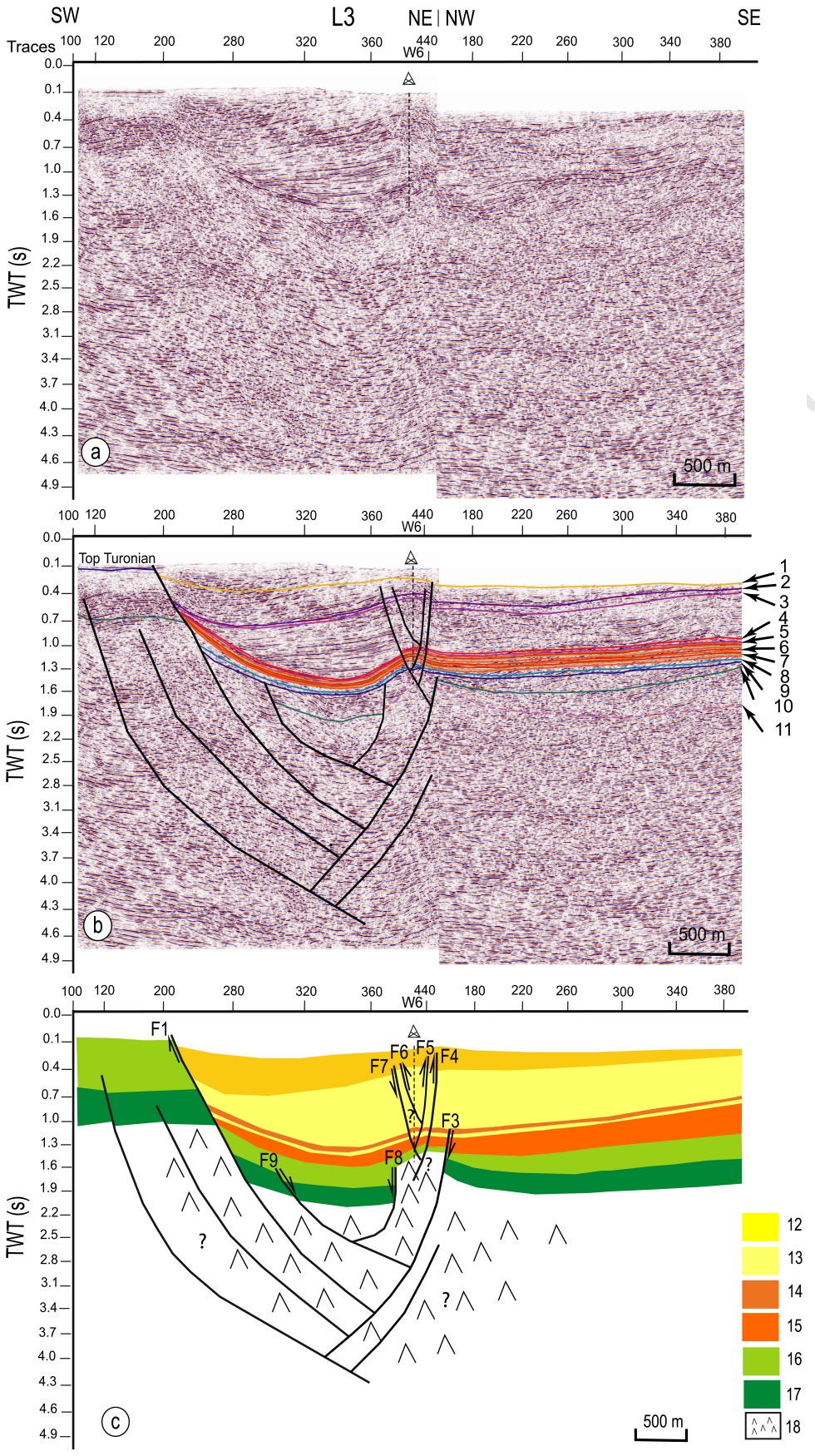
SW
L3
NE | NW
SE
Traces
100 120 200 280 320 360 440 180 220 260 300 340 380
W6
TWT (s)
0.0 0.1 0.4 0.7 1.0 1.3 1.6 1.9 2.2 2.5 2.8 3.1 3.4 3.7 4.0 4.3 4.6 4.9
a
500 m
Top Turonian
1 2 3 4 5 6 7 8 9 10 11
b
500 m
F1 F2 F3 F4 F5 F6 F7 F8 F9
?
12 13 14 15 16 17 18
c
500 m

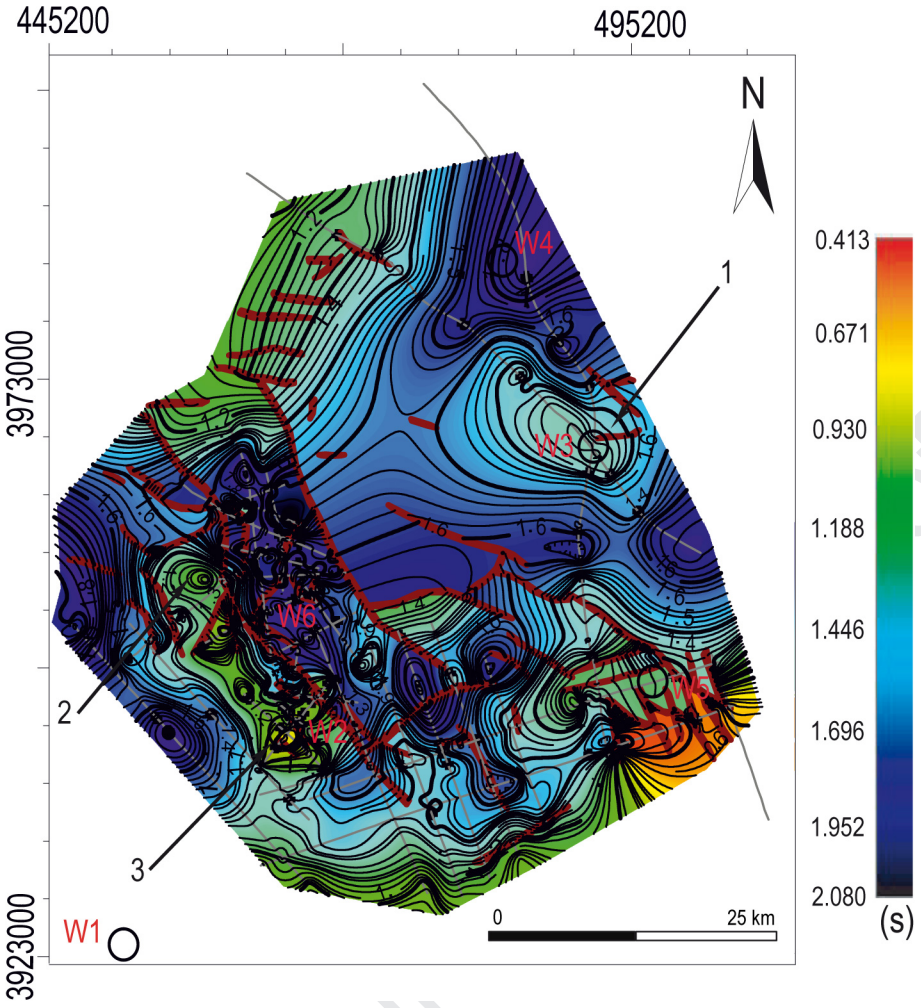

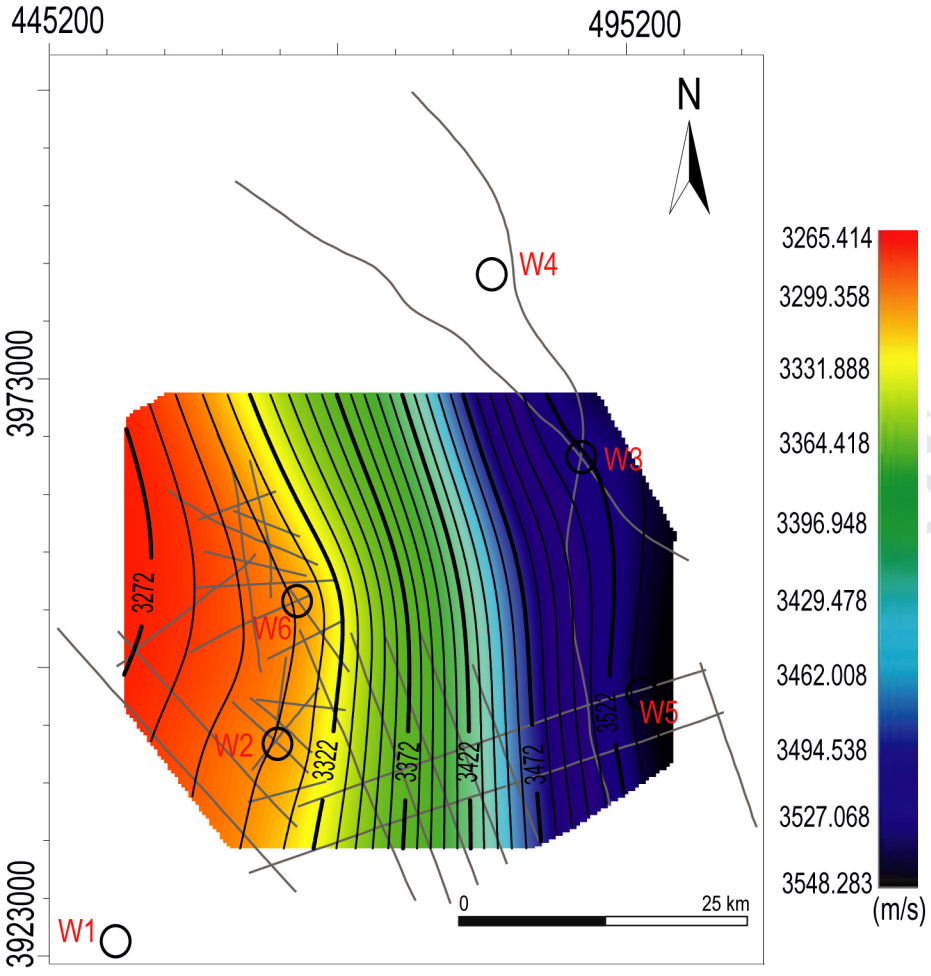
445200
495200
N
3973000
3923000
W1
W2
W3
W4
W5
W6
3272
3322
3372
3422
3472
3522
0
25 km
3265.414
3299.358
3331.888
3364.418
3396.948
3429.478
3462.008
3494.538
3527.068
3548.283
(m/s)

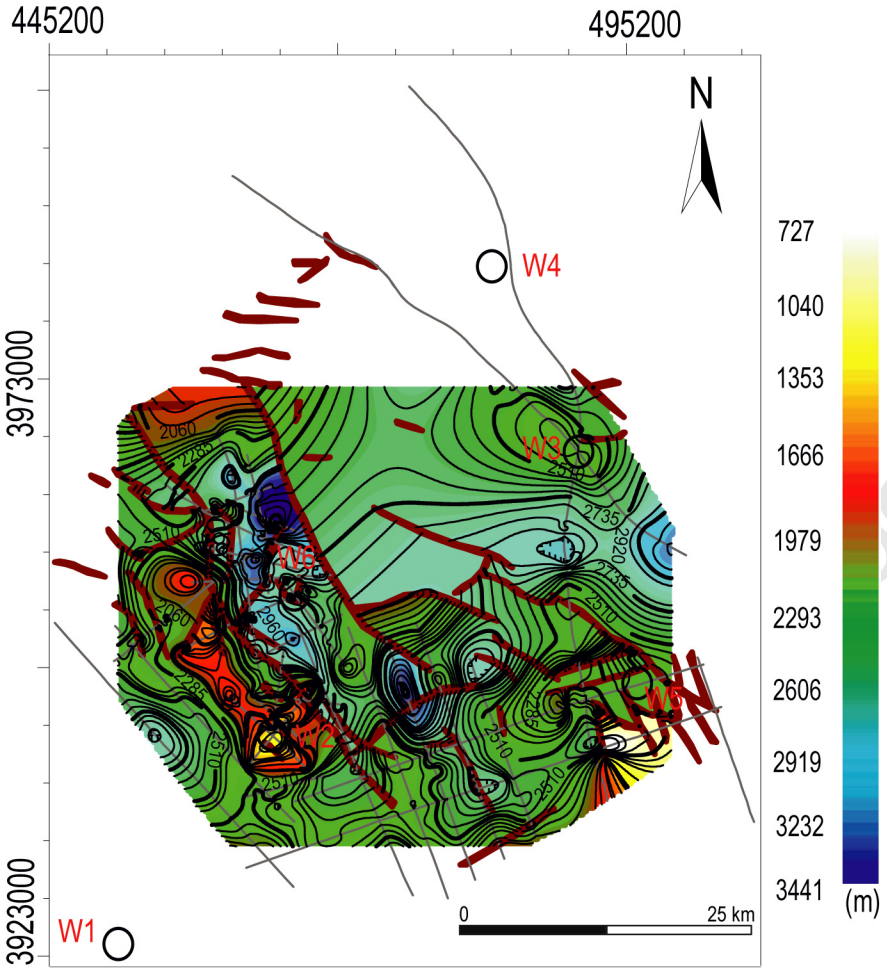

Highlights

- The Cenozoic cover appears through development of “pull-apart” basins of variable sizes and shapes as a consequence of ~N160° shortening.
- The NW-SE, NNW-SSE to NS and NE-SW to E oriented fault network developed during Mio-Plio-Quaternary.
- Well logs, 2D seismic lines and gravity data indicate the role that such faults may have played during the fast subsidence and sedimentary infill.
- A fold-fault beneath well W6 within Kalaa Khesba Graben is evidenced by the triggering of dextral EW strike-slips.
- N160° Mio-Plio-Quaternary Transpression may have (i) controlled the distribution in thickness (0.5-4 km) and facies of Meso-Cenozoic stratigraphic sequences, (ii) induced the duplication of productive Paleocene-Eocene series with subsurface push-up inversion structure.